Department of Precision and Microsystems Engineering

Fusion of smart material and compliant mechanism
A study of piezo-flexure hinge

Tian Luo

Report no	: 2017.017
Coach	: Dr. Hassan HosseinNia
Professor	: Prof. Just herder
Specialisation	: Mechantronic system design
Type of report	: Msc Thesis
Date	: 30th March 2017

Preface

This work is part of Msc thesis program of Tian Luo and is dedicated to fulfillment of the requirements for the degree of Master of Science of Mechanical Engineering at Faulty of Precision and micro system engineering of Delft University of technology (TU Delft) , with specialization in Mechantronic system design. This research has been processed under expert guidance and supervision from specialist at TU Delft.

Tian Luo
Delft, March 2017

Acknowledgment

I would give my biggest thanks to everyone who helped me in my final year as a student. Life is good, life is bad, everyday we meet a new world and new challenges. There is no reason for us to stop and get lost. However people meet troubles, get stacked, fortunately, we have our families, friends and supervisors on our side, in those difficult days, it is them who help and encourage us get one step further and face the challenges.

Special thanks goes to Dr Hassan for for his constant expert guidance and supervision and To everyone I met in delft, thank you a lot for making these years colorful and wonderful.

Contents

1

Abstract

Machines are widely used all around the world, they are powerful but still limited by some problems. Endless conflict between growing needs of versatility and unbearable complexity seriously restricts development of modern machines.

To solve this conflict, one way is to improve setup integration, since system complexity is very sensitivity to components‘ weight. In order to achieve the goal of improving system integration and enhance performance, a new hinge design with piezo-flexure is proposed in this report. This design makes use of both smart material and compliant mechanism to achieve a highly compact structure.

In this project, a prototype has been built and tested in both simulation and real experimental environments to validate this hybrid hinge design. According to identification results, this hybrid design meets several problems from piezoelectric material, nonlinearity as well as electricity coupling among all instruments give this hinge design very unique response features. In order to handle these problems, a controller with feedback, feedforward and disturbance observer has been built to ensure performance of this kind of piezo-flexure hinge.

With this dedicated controller configuration, piezo-flexure hinge shows nice performance in both precision and speed.

2

Introduction

2.1. A brief problem review

Machines are powerful and they are getting stronger faster and smarter everyday, but they do meet a lot of challenge, and system complexity is one of the most serious problems. To achieve a vivid mechanism design, the most common principle is to have more controlled DoF, as a results, on one hand, as advantages, this mechanism can achieve a high mobility, flexibility and controllability , on the other hand, as disadvantages, system complexity is also highly increased. High complexity means that there are large amount of joint, actuation and necessary components. This complexity will not only increase design difficulty, but also increase total weight of the whole design. Unfortunately, multi-stage mechanisms are very sensitive to the weight issue.

Consider a three stages manipulator which is in the most common configuration as a example, every stages are connected in series with actuators placed between two adjacent stages. If the weight of stage I is increased, to maintain the desired payload manipulability output of actuator I needs to be enhanced, however, extra weight always comes with extra output, and the actuator II must be further enhanced to deal with both extra weight of stage I and actuator I at the same time, as a result actuator II becomes much heavier, and the same story will also go to actuator III. Besides to hand these heavier actuators, stiffness of these stages also need to reinforced, which will cause even more extra weight. In the final end, an increment of one stage results in a much larger increment of the total weight, and things will be even worse if there are even more stages. This chain reaction among all these stages explained why a machine needs to be a jumbo size to move a tiny object.

In space nonsensitive environment, like an iron plant, this size is acceptable, but there are more environment that are sensitive the total size and weight or even the outlook of a machine, for instance, a surgery machine that are highly functional but not fit size of human body will never be accepted by any hospital. Besides, machines in people‘s life are even much sensitive to machine size and weight, because they have to fit in the size range of human body. For example, vivid robot hand, a promising candidate for future human-computer interface, has to be achieve more than 10 controlled DoF in a size a human‘s hand.

Conflict between functional and geometric requirements does limited the development of machine design. To solve this problem and satisfy requirement of these size weight sensitive environment, one way is to move all these actuators to the base and use an additional power transmission system to transmit the driving force from actuators to their corresponding joints, so that a larger and heavier actuator will not cause a chain reaction among all structure and ruin the whole machine with unacceptable weight and size requirement. However this kind of solution still has its own shortcuts, that is, when there are too many stages, efficient of the transmission system drops rapidly, in that condition, increased weight of the transmission system will no loner be negligible while the difficulty of designing and manufacturing such a complex transmission system will ruin the machine in another way.

An alternate solution is to optimize the actuator, by improve the integration of each stage, by making it

more compact, weight could be saved on each single stage and due to the chain reaction, much more weight of the whole machine could be saved. A conventional pin joint which are widely used in multistage manipulators is usually driven by an on-joint actuation, which means that the actuator is placed at the position of corresponding joint. This kind of design is compact in size, but still heavy in weight. To improve performance of a pin joint, introducing compliance mechanism and smart material to this conventional hinge could be a very promising solution.

2.2. compliance mechanism

Compliance mechanism is kind meachanical design that make use of the deflection of mechanism parts to achieve a desired motion. A compliance joint usually uses so called flexure, a thin metal plates, to lock some DoFs of the object, so that the object can only moving in the desired directions. Typical compliance mechanism structures are shown in figure below.

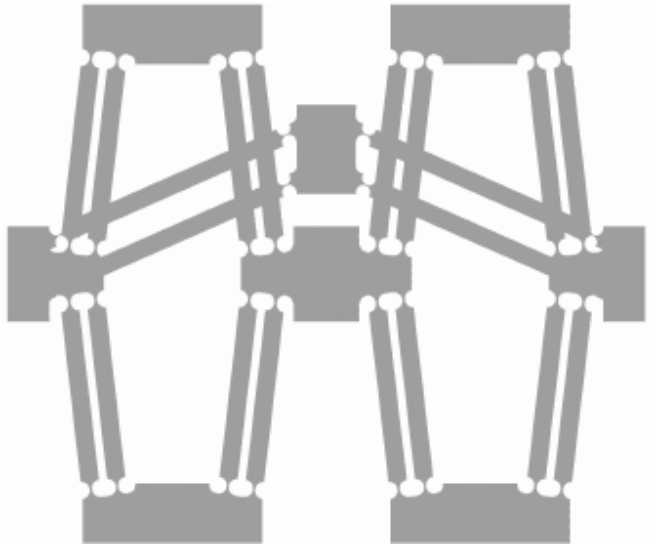

Figure 2.1: A typical compliance mechanism

Since this mechanism only make use the deflection, not relative motion between two components, no lubrication is need, hence a bearing or a lubricant groove is no longer needed, weight of this part can be easily saved and the structure complexity is also reduced due reduced number of components. Besieds, total weight of these thin plates are usually smaller than that of a thick pin in the pin joint, which also save some weight.

If implement compliance hinge in to a multi stage machine to replace conventional pin joints, weight could be saved, the these saved weight will be also amplified by multi stage structure. So that, even it is only a small reduction on the joint weight, the total weight of the whole structure could be significantly reduced. What‘s more, when these pin joints are replaced by compliance hinge, a lot bearing and lubrication stuff can also be removed, hence the complexity is reduced and repairability is improved.

2.3. Piezoelectric effect

Piezoelectric effect is kind of material feature, for those piezoelectric material, when source is connected to the material, voltage will force atom cell inside marerial, rearrange in space. Then rearranged atom distribution will generate inner stress, and finally results in deformation in a macro scale.

A piezoelectric actuator can make use of this effect [1], by well arrange orientation and distribution of this material, when an external voltage presents, the whole material body could deform in the desired way

to achieve a desired motion. because the force is almost uniformly generated along the whole material body, piezo actuator is also called distributed actuator.

Piezoelectric materials are mainly concentrated in two category, that is, soft piezo foil and hard piezo ceramic, working principle of them are similar. Piezo material actuators can usually generate a relatively high force force output, but as a compromise, it need a high operation voltage, usually beyond one hundred of even one thousand.

Because force output comes from the material itself not from a structure, like the coil in a motor, it becomes possible to adjust shape of a piezo actuator depending on different working requirement, this feature gives piezo actuators huge flexibility in complex working environment.

Among all kinds of piezo actuator, piezo bender is a popular configuration. Usually a piezo bender is configured with two layers of piezo material stacked together, the two layers working in different way, when voltage is added, one of it will expand, another one will shrink, as a result, the whole bender will bend. If the voltage is inversed, respecting motion will also be inversed and the bender will bend to another direction. But due to anisotropy of piezo material, bender response is slightly different in two moving direction.

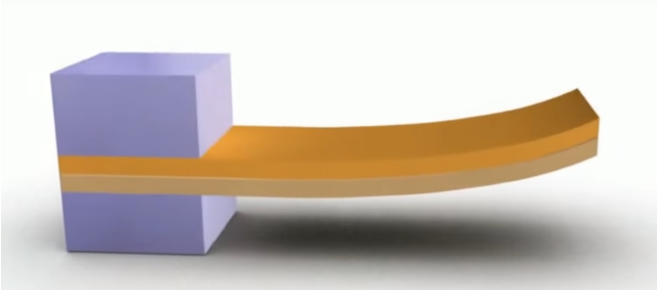

Figure 2.2: A typical piezo bender configuration

2.4. Project goal

Using compliance mechanism already improves performance of a machine with multi stage structure, but there is still a possibility to achieve a even better result, that is, applying distributed actuation directly on flexure to replace external actuation. Because in common case, compliance hinges are only used as a suspension component, external actuation unit is need to drive the whole mechanism.

As mentioned in previous section, for a multi stage machine, improving integration can easily improve overall performance, if the external actuators can be integrated on the flexure to achieve an on-joint actuation, system integration can be greatly improved, and machine can reach a even better performance, lower complexity and higher reliability. To achieve an on-hinge actuation, applying smarter material is a very promising choice because of its high compatibility flexibility.

Task of this thesis project is concluded as to give a high performance solution for the idea of fusing smart material and compliant mechanism together. And this task can be divided into three main parts.

Concept design To merge the function of smart material actuation and compliant mechanism suspension together, a special mechanical configuration has been proposed and simulated to match new requirements of this compact design.

Prototype building and identification To Validate the concept design, a prototype of piezo-flexure hinge has been built and tested to check mechanical behavior as well as electric compatibility

Control design To achieve a high performance hinge design, a special controller setting has been built for this special hybrid hinge to compensate nonlinearity of smart material and compliant mechanism.

These three sub tasks and corresponding results are elaborated in following chapters.

3

Compliance hinge design

Flexibility gives compliance huge advantages over pin joint in environment sensitive conditions. To achieve a single moving motion, multiple kinds of flexure configuration could be implemented to meet the same goal in different ways and satisfy different geometric constrains. In this thesis, design constrains are not coming from requirements of the complex task, but from fusing piezo and flexure together. In this chapter, several types of configuration are proposed and tested to validate the idea of fusing piezo and flexure together,ceramic type piezo is at first priority in this design process. To study property of these fused structures, finite element method is used to analyze them, with help of this method, before making test prototype in real word, both static and dynamic features of candidate design could be simulated in softwares, and hence the design process could be much rapid and vivid. To do the FEM analysis ANSYS FEM software is used in this chapter.

3.1. Basic features of compliance hinge

Even a fused piezo-flexure structure is so multi-role, most of its mechanical features follows that of a normal conventional metal compliant hinge with the same shape. So in this section, before fusing piezo and flexure together, a basic and simple compliant hinge is tested to have preview of many key features, such as stiffness, stress condition, of a compliant hinge.

3.1.1. Hinge configuration

A compliant hinge with butterfly structure as shown below in figure 3.1, is used in this section, detail geometric data is listed in appendix. It is the most basic configuration of a single DoF compliant hinge, which only uses two pieces of flexure to form a cross configuration. This type of hinge can only rotate around the center of the cross and has highly anisotropic stiffness.

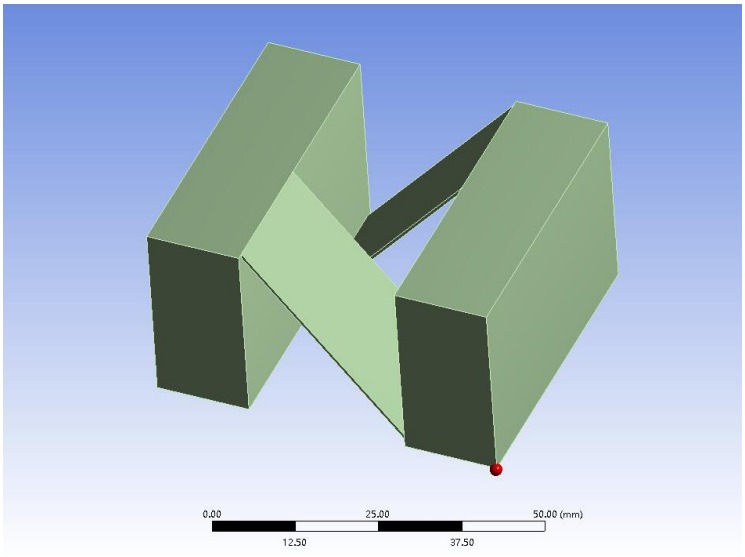

Figure 3.1: Basic butterfly configuration

3.1.2. FEM analysis

FEM model First is to build the mesh network on the CAD model, considering that the two mass blocks are stiff and few deflection will happen even under a huge force load, only few elements are needed in that domain, hence, element size of these two blocks is set to $2mm$. Meanwhile, deflection of compliant hinge mainly happens on the two plates and these plates itself is also a thin shell structure, element size should be much smaller compared to that on the mass block, and the size in thickness direction should be even finer, hence, size of the flexure is set to $1mm$ to reinforce calculation precision.

The meshed model which contains is shown in figure 3.2below.

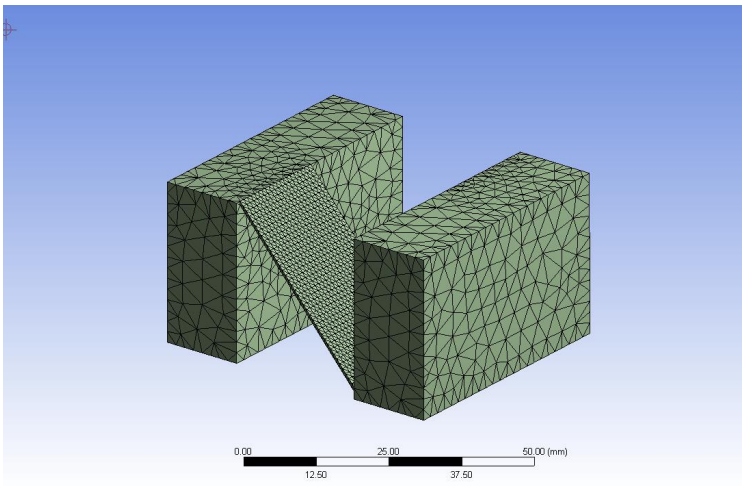

Figure 3.2: Mesh network of FEM model

Both the mass blocks and thin plates are set to be made of stainless steel, like as normal configuration, mechanical specs are list in appendix

Stiffness of the hinge To analyze stiffness of the hinge, multiple moments in different direction are loaded on the right surface of the right mass block, while the left surface of the left mass block is totally constrained,

configuration is also shown in figure below. This figure only shows a moment in X direction as example, simulations have been processed in both three direction.

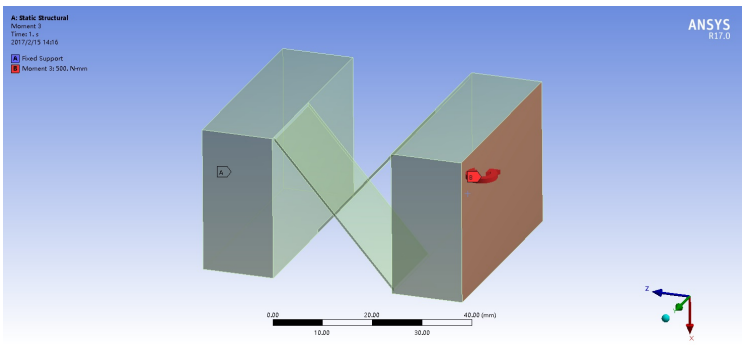

Figure 3.3: Load and constrain condition

Magnitude of every moment is set to $0.5Nm$. Bending deflections are shown in figures below.

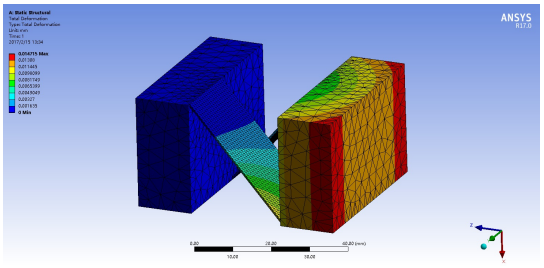

(a) Deflection under x-direction moment

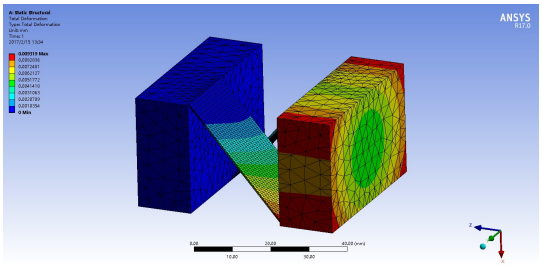

(b) Deflection under y-direction moment

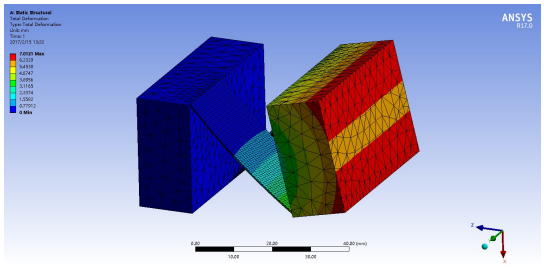

(c) Deflection under z-direction moment

Figure 3.4: Deflection of the basic compliance hinge

According to the simulation results, it is clear to see that stiffness of this hinge is highly anisotropy.

Eigen mode and eigen frequency Eigen mode and eigen frequency are important in any dynamic response analysis, as they can not only indicate system performance when a reference signal is added, but also the control potential of the setup. In this section, the eigen mode is obtained when the left surface of the left mas block is totally constrained. Eigen frequency of the first four eigen modes is listed in table

Mode	Frequency(Hz)
1	26
2	527
3	725
4	1802

and Shapes of these modes are shown in figure 3.5below.

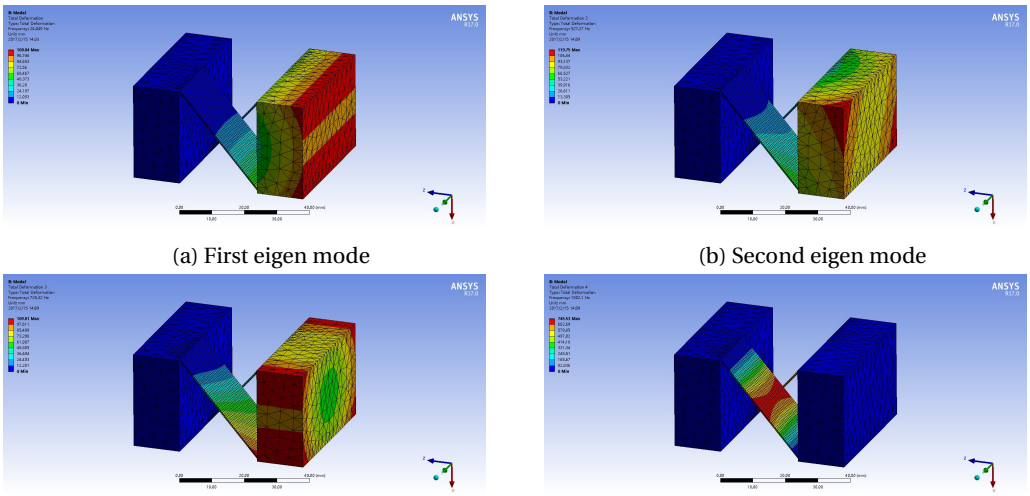

(a) First eigen mode

(b) Second eigen mode

(c) Third eigen mode

(d) Forth eigen mode

Figure 3.5: Shape of eigen modes of this compliance hinge

3.1.3. Conclusion

Compliance hinge itself is a very nice hinge structure, it is not only weight efficient, but also can provide a very nice mechanical property. The first eigen frequency is very low among all the first 4 eigen mode, this difference gives compliant mechanism a big advantage in control design, since, in normal working frequency range ,only few eigen modes will involved. Second is that stiffness of a compliant hinge is so anisotropy that the structure can attenuate or reject force or moments comes from different directions.

3.2. Fusing piezo and metal flexure

In this section piezo bender and metal flexure is implemented in a compliant mechanism with butterfly flexure configuration and piezo patch benders are directly stacked on the flexure surface. [2] [3].

3.2.1. Model design

The model is shown in figure below, detail geometric data is listed in appendix.

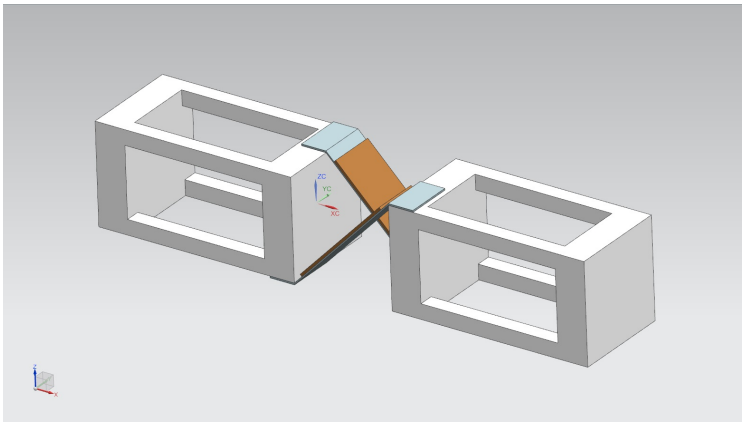

Figure 3.6: A fused piezo flexure hinge configuration

The white parts are frame gray parts are metal flexure and the brown parts are piezo bender. Design idea of this model is simply adding a piezo bender on the metal flexure, [4] so this flexure will play two role in this design, first is acting as connecting piezo and the two frame together. The second is acting as substrate of piezo bender. So, when voltage is added, piezo bender will be activated and drives a bending motion on the flexure, finally the whole joint begins rotating. Generally, a typical piezo bender is a sandwich structure, a piezo ceramic layer covered by a plastic coating on each surface. However, stiffness of piezo ceramic is much higher than that of plastic coating, hence, mechanical feature of a piezo bender is dominated by the feature of piezo. To simplify this problem, this sandwich structure is reduced to a single layer one.

3.2.2. FEM anlysis

FEM model Compare with the thin flexure or piezo bender, these two frames are stiff and strong, so relatively larger element size is used in this two components. When the piezo-flexure hinge is activated, deformation and stress will strongly concentrated on both piezo and flexure, to achieve a higher working precision, a fine mesh network is used on these parts, besides, considering that stress distribution in thickness direction is also interested, element size in thickness direction will be further reinforced [5]. so element size of frame is set to $1.5mm$, of piezo and flexure is set to $0.5mm$ in planar direction, while $0.1mm$ in thickness direction. Meshed model is shown in figures below.

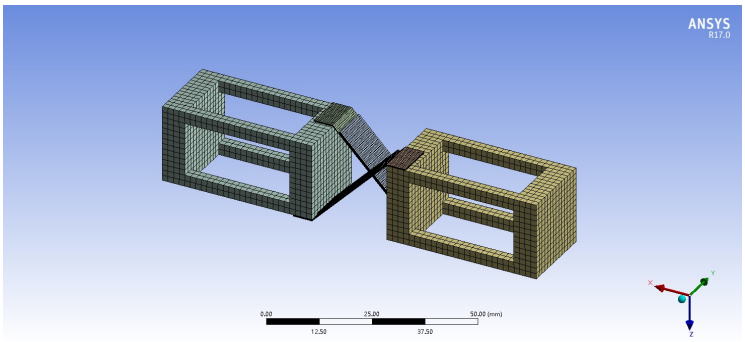

Figure 3.7: Mesh network of a piezo flexure hinge

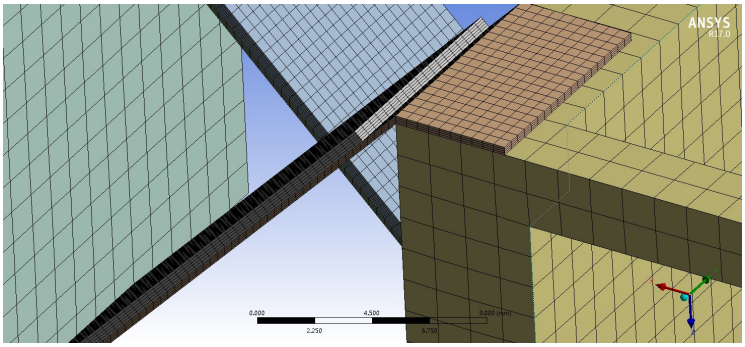

Figure 3.8: Mesh network of a piezo flexure hinge

Material of frame and flexure is set to be stainless steel while these piezo is set to be piezo ceramic PIZ 255.

Load and constrain To study behavior of a piezo-flexure compliant hinge, first is to simulate the behavior of the piezo bender.

When voltage is added to a piezo bender , due to its special material orientation configuration,material on the top surface will expand while the bottom surface shrink, as a result of these two motion, the piezo plates

begins to bend. In this way, stress distribution is similar to that of a beam under pure bending moment. So in this section the distributed force generated by piezo bender will be replaced by a pair of bending moment.

So, to simulate behavior of this piezo flexure compliant hinge, loads and constrains are added as shown below. the right surface of the right frame is fixed, and two pairs of $1.2Nm$ bending moments are loaded on the two side surface of the two piezo benders.

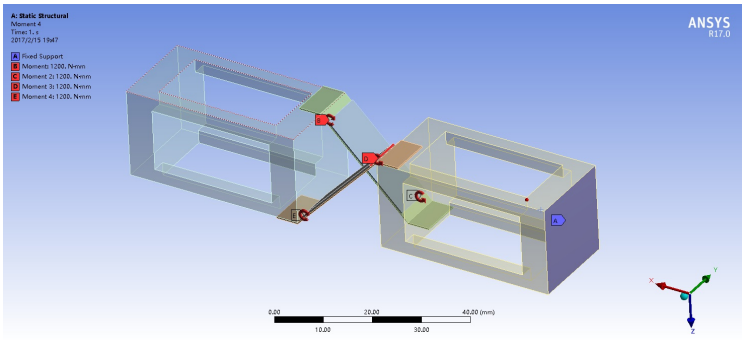

Figure 3.9: Load and constrain condition of hinge motion study

Hinge motion Response of this compliant hinge under such a load condition is shown in figures below. A 0.5× scale is implemented in this drawing.

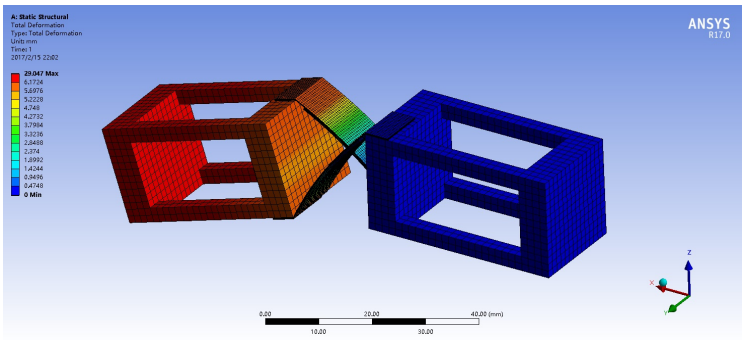

Figure 3.10: Hinge response under bending moments

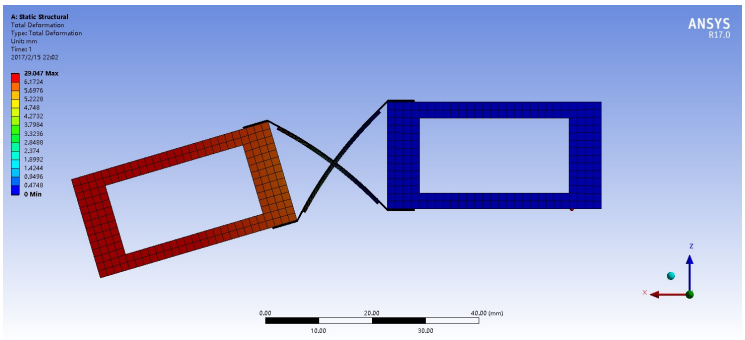

Figure 3.11: Hinge response under bending moments

According to the simulation results, this type of configuration can generate a relatively large motion that match the basic requirement of a hinge design,

Stress condition Stress distribution of this load condistion is shown in figures below, A 0× scale is implemented in this drawing.

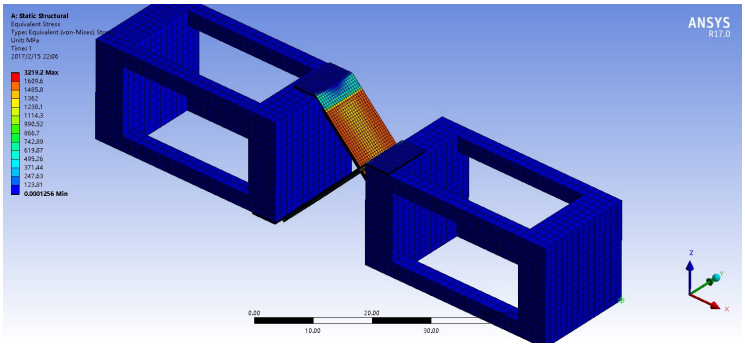

Figure 3.12: Stress distribution of the whole design

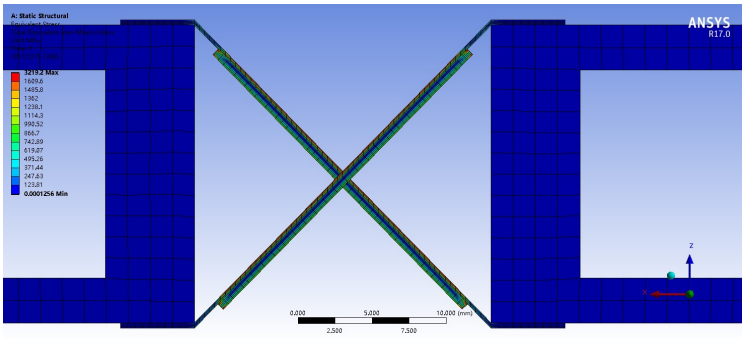

Figure 3.13: Stress distribution of the fused piezo-flexure side view

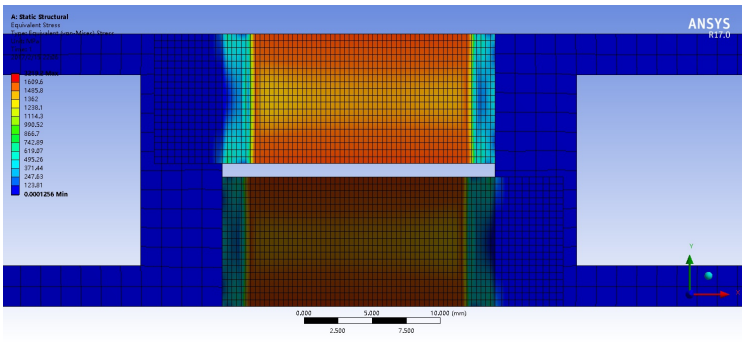

Figure 3.14: Stress distribution of the fused piezo-flexure top view

Eigen mode and eigen frequency Eigen mode and eigen frequency is obtained by fix the right surface of the right frame, results are shown in table and figures below.

Mode	Frequency(Hz)
1	19
2	253
3	781
4	1147

and Shapes of these modes are shown in figure 3.5below.

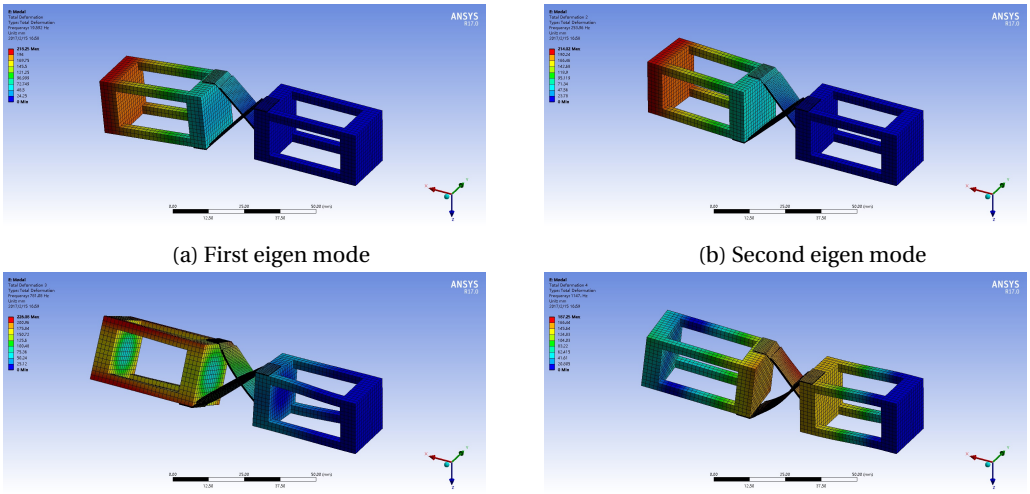

(a) First eigen mode

(b) Second eigen mode

(c) Third eigen mode

(d) Forth eigen mode

Figure 3.15: Shape of eigen modes of this compliance hinge

According to the analysis results, the first eigen frequency is much lower than second eigen frequency, which match prediction made in basic structure study section. Due to this huge gap between first and other eigen mode, this design has very nice control potential. However, the low first eigen frequency may limit system bandwidth.

3.3. A compact prototype design

Previous analysis shows great potential of compliant mechanism being used in hinges and validates the possibility of fusing piezo and flexure together, however when building piezo-flexure compliant hinge in real word, there are much more thing that need to be conclude in design process rather than drawing in softwares. Components manufacturing, cable wiring and piezo-flexure fusing.

3.3.1. Model design

Because the pizo bender built with piezo ceramic material has almost the same young‘s module of steel, instead of sticking a piezo bender on a metal flexure, those flexure are completely replaced by a piezo bender. In this way, the design could be even more compact. However, it also results in some disadvantage, without metal flexure acting as connecting component, the frame block and fixing methods need to be modified to directly connect piezo bender to the frames. one solution is shown in figure below. Detail geometric data is listed in appendix.

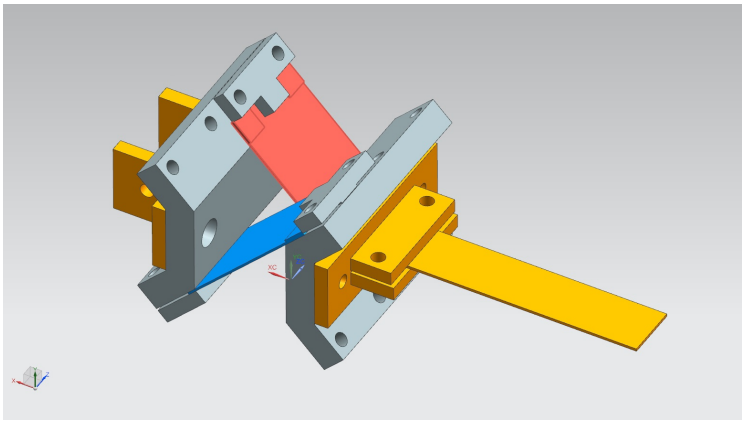

Figure 3.16: A compact piezo-flexrue hinge design

The brown parts are piezo bender while these white parts are frame with their sharp edge replaced by slopes surface, so that this piezo benders can glued or bolt fixed on this slopes. Because this design is a candidate one for prototype building, connecting and measurement components are also include in this model.

3.3.2. FEM anlysis

FEM model These frame and clippers are much stiffer than the three thin plates, so a coarse mesh is sufficient, hence element size is set to $4mm$ in these domain. Although the beam used in measurement purpose is thin, its deflection is not interested in this chapter, a coarse mesh network with element size equal to $2mm$ is built on this beam. Deformation mainly happens on the two piezo benders, so that a fine mesh network is used, element size in this domain is set to $2mm$. The completed mesh model is shown in figure below .

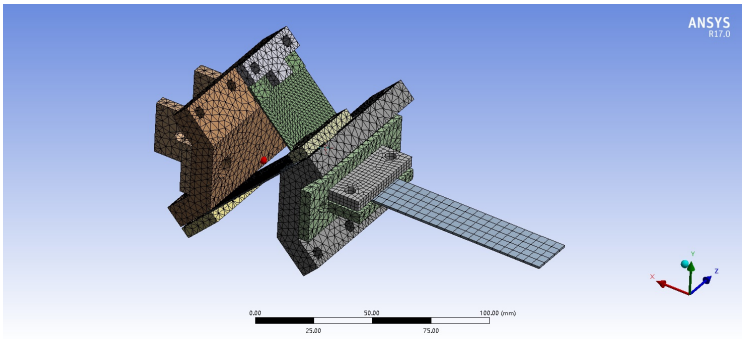

Figure 3.17: Mesh network of this compact design

Loads and constrains Loads and constrains are added as shown in figure below

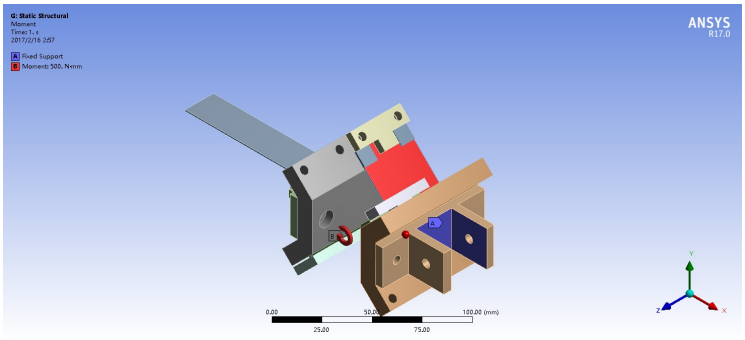

Figure 3.18: Simulation loads and constrains condition

One side of the hinge is totally fixed, while four bending moment with magnitude of $0.5Nm$ is added to the surface of the two piezo bender.

Hinge motion Under such bending moment, hinge response is sown in figure below.

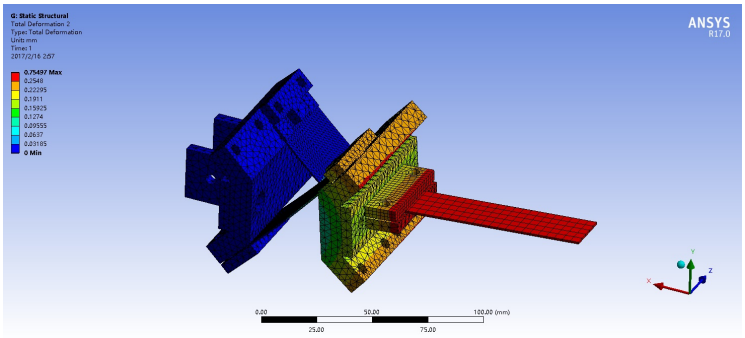

Figure 3.19: Simulation loads and constrains condition

As we can see in this figure even the flexure-piezo hybrid structure is replaced by a single pieces of piezo, due to similar mechanical property , response of this model is very similar to previous models. With a bending moment, the hinge begins to move.

Stress distribution Strees analysis is also based on motion mode used in last section, analysis results are shown below.

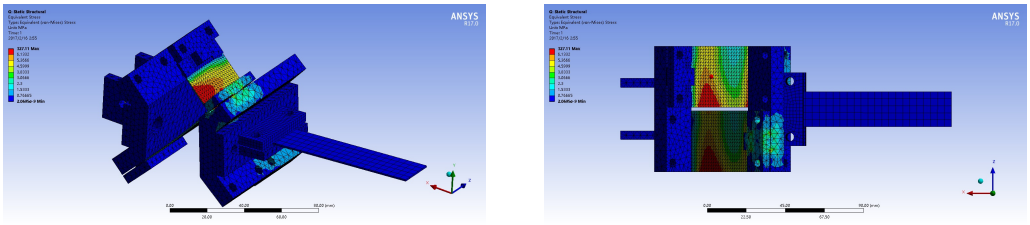

(a) Normal view (b) Top view

Figure 3.20: Stress distribution on the compact model

Eigen Models and eigen frequency The first 4 eigen model are captured almost in the same way as what is used in previous sections one side of the structure is fixed, while the other side is free. Eigen mode and eigen frequency is obtained by fix the right surface of the right frame, results are shown in table and figures below.

Mode	Frequency(Hz)
1	19
2	253
3	781
4	1147

Shapes of these modes are shown in figure 3.21 below.

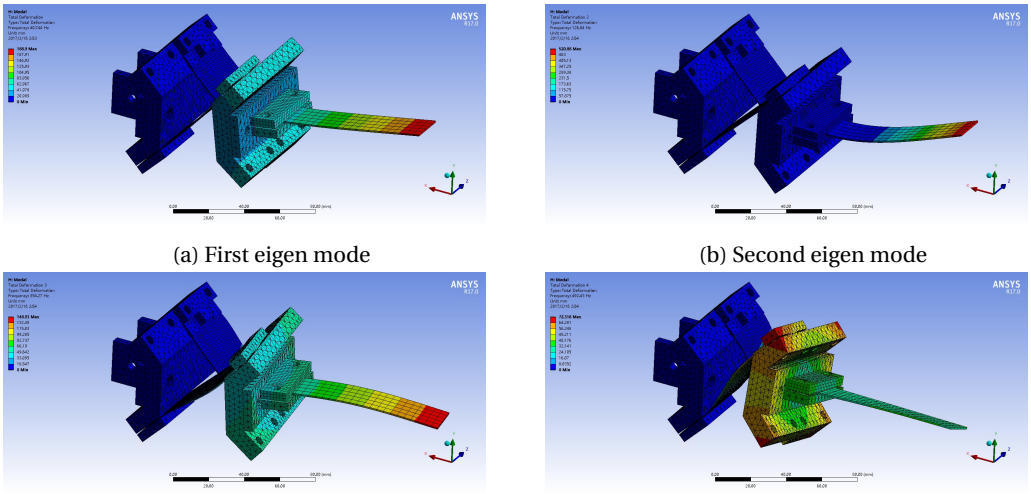

(a) First eigen mode

(b) Second eigen mode

(c) Third eigen mode

(d) Forth eigen mode

Figure 3.21: Shape of eigen modes of this compliance hinge

Frequency of the first eigen mode is still far away from other eigen modes, but the gap between the first and second one is smaller compare with other configuration. It is because that the second peak is caused by the beam bending of the measurement parts. In real practice this part will be replaced by a stiffer frame, which will significantly rise frequency of the second eigen mode. So affect of the second peak could be ignored in next steps.

3.4. Conclusion

Three models are studied with FEM in this chapter, these studies indicates that its very helpful to have a brief preview of a metal compliant hinge prior to fuse piezo and metal flexure together, as a piezo-flxure almost follow the same mechanical property of the same shape pure metal structure. So that, piezo -flexure compliant hinge also inherits both advantage and disadvantage of compliant mechanism

For piezo-flexure hinge, they usually have much lower first eigen frequency, on one hand the huge gap between first and other eigen frequency makes the control mode much easier. on the other hand, a low eigen frequency may limit the over all performance of a piezo compliant hinge. To achieve a optimal design, it is very necessary to balance this pro and con. Thanks to the flexibility of flexure compliant hinge, the eigen frequency could adjusted by modified configuration of flexure amount or shape.

Because a compliant hinge takes advantage of flexure beam bending motion to achieve a over all rotation, when the motion is large , the whole hinge is not linear, first is that the rotation center will shift due to shape change of flexure.

4

Prototype building and testing

Setup in real world involves much more external disturbance source than in simulation. For assembly error, small difference among each same type components, coupling between amplifier and piezo materials are hardly calculated in simulation but can easily affect real setup performance. Considering this condition, system identification becomes the best choice to a deep and detail study of a mechantronic setup. By calculating and analyzing relationship between input and output signal, detailed dynamic features of the tested system could be captured.

4.1. Peizo bender test

4.1.1. Introduction to piezo bender

In this thesis, two types of piezo bender is chosen as potential candidates, which are A15 and 12 from PI company. Specifications of these two piezo actuators is list in appendix. For those piezo bender, they are made of piezo ceramic plate and covered with plastic coat. specifications of piezo ceramic is listed in appendix. the material is configured in bending actuator model, so when voltage is loaded to the piezo material, piezoelectric action will first generate stress difference between top and bottom surface of piezo material layer, then the stress will force the actuators perform a bending motion.

Because of using ceramic material, these two actuators gain very helpful mechanical feature, it is much more stiffer than piezo foil, so itself could take the role of metal flexure in compliance mechanism. Then overall structure could be much more compact than piezo foil design which has to companion with extra metal plates.

Whats more is that the overall stiffness of this kind of piezo bender is similar to aluminum, so preliminary of metal compliance mechanism design could be used in this thesis and improve design effect ion.

4.1.2. Test setup

In this section,response features of these two piezo benders are identified. Experimental setup is built as shown below, detail dimensions are list in appendix.

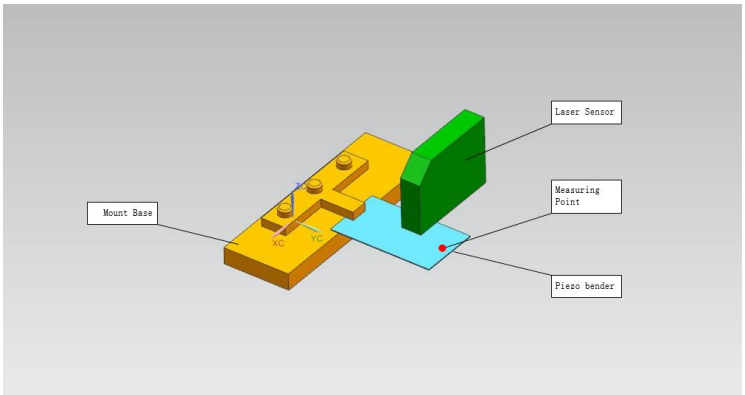

Figure 4.1: Piezo bender identification setup

Piezo bender is clamped on a metal base while a laser sensor is used as a touch-less displacement measuring device to measure displacement of the measuring point. Input signal of identification process is generated by a measuring Box by National Instrument. This signal is then amplified by an amplifier XXX by smart-material, technical specs of these two equipments are listd in appendix XX. The amplified signal is finally loaded on the piezo bender. Under a external voltage signal this piezo bender will begin to bend, and this bending motion is measured by LASER sensor. Output signal of this LASER sensor is current whose magnitude is proportional to the deflection magnitude with an constant offset. This output signal is obtained by measuring the voltage on a certain known resistor when the output current is going through it. Voltage on this resistor is also measured by the NI measurement box used in signal generation. Schematic figure is shown below.

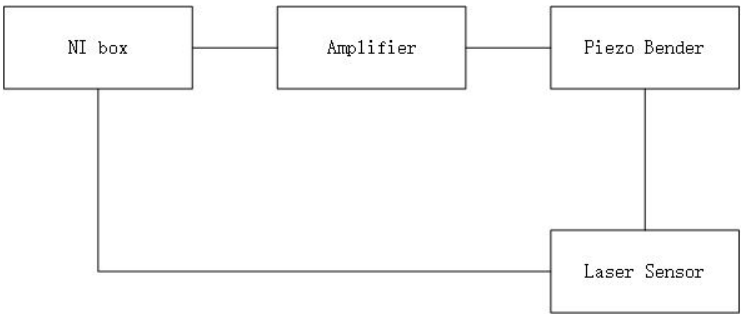

Figure 4.2: Electronic device connection graph

Before piezo bender identification process, this amplifier is tested without any working load, that is, piezo bender will not be connected to the amplifier, output of the amplifier is shown in figure below in spectrogram form.

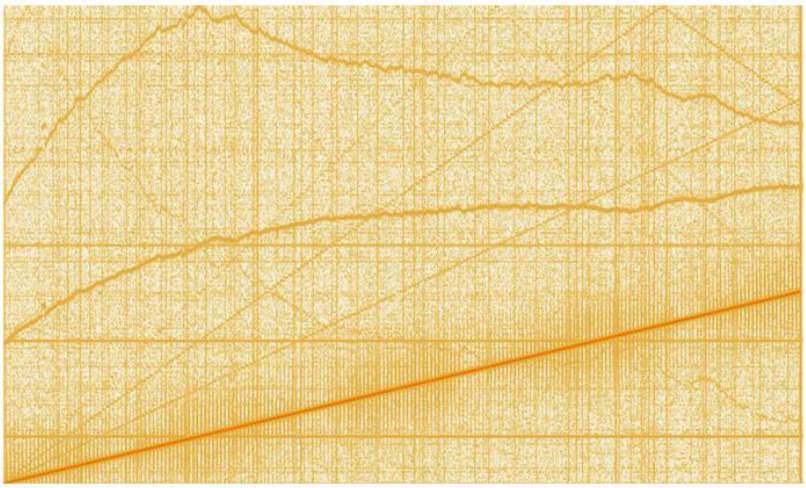

Figure 4.3: Spectrograms of zero load test

According to spectrogram of zero load test, the amplifier used in this project is not very good, it meets several disturbance source as well as significant harmony effect, these imperfectness need to be carefully considered in next research progress since they will reduce setup performance. So piezo bender test and identification will focus on 3 main features as listed below.

- Static response
- Dynamice reponse
- Hysteresis

For Static analysis, input signal changes slowly from the lower bound to the upper bound of the tested piezo bender.

For Dynamic analysis, NI box generates a sinusoidal wave at $1Hz$, after every 3 seconds, signal frequency increases by $1Hz$, at the same time, the measurement box is continuously measuring the output at $1000Hz$. Here, using a very discrete frequency rather than continuous sin-sweep signal is mainly because of the short-cut of NI measurement box, this kind of box can only make a perfect frequency change when the changing poing is at somewhere the signal is exactly at $0V$ or a amplitude shift will happen, what's worse, this shift will take an unforeseen time. this two backwards will finally give more unfriendly noise to the test setup and reduce accurate of test results.

Because the measurement channel is running at $1000Hz$ and the measurement process stay at a certain input signal for 3 seconds, according to Nyquist principle, frequency measurement range is between $0Hz$ and $500Hz$, while resolution is about $0.33Hz$. After obtaining necessary test data, post-process is necessary before analysis, DFT is mainly used in this step, thanks to the discrete input frequency of input signal, DFT window size and overlap size become an easy problem, which will be individually chosen for different analysis purpose and experiment setup to increase analysis precision.

It is very important to notice that piezo material is a kind of capacitive device, which means that the higher frequency signal is loaded, the lower impedance the overall circuit will be, eventually, the higher current will appear on the output port of amplifier, This shortcut will limit measurement range of dynamic test range.

For hysteresis analysis, process is similar to previous static analysis, input signal changes between upper and lower limit, with a relatively higher speed comparing with static analysis.

4.1.3. A15 piezo

Static response
Piezo material has some very special features compare with normal metals, which would make the piezo bender show some unique response. In this step a slowly changing step wave signal is given to the system, because it changes so slow, system could be regarded as always steady state.

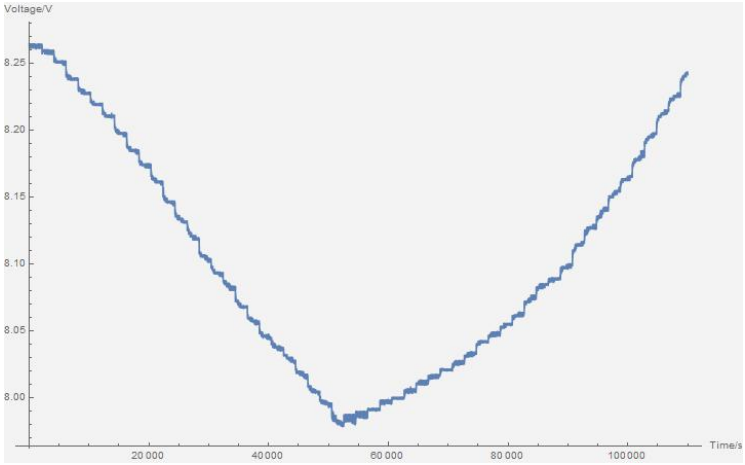

Figure 4.4: A15 piezo response under a slowly change step wave

it is necessary to mention that the resolution of sensor is low, which makes system response in time domain looks discrete. roughly plot of the the experiment looks like a system with hysteresis. However if zoom in to the step detail, unique features could be seen, which are shown in figure below.

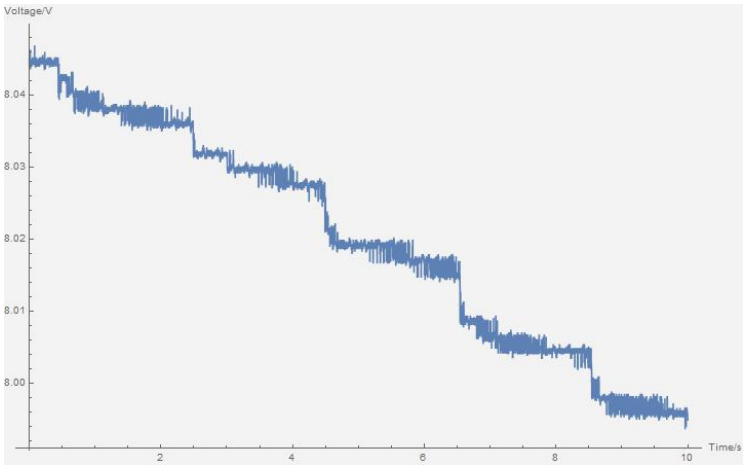

Figure 4.5: Piezo releasing phenomenon on A15 piezo

According to figures above, we can see that piezo bender first reach position A and then struggle to another position, in some case, piezo bender even jump to a third position. This very unique feature of piezo bender is because that piezoelectric material will release after reaching a position due to charge re-distribution, which means that even if a constant voltage is applied, piezo material will not go to a constant position. And this kind of response is depended on offset level and step size.

Because this coming back motion only happens in steady state and will not take place immediately, it becomes difficult to be captured in time domain identification, where the input signal is always changing and system will never reach a steady state and releasing. As a result, accurate of the identified system at very low frequency range becomes lower. Besides, even the real gain is not a constant number, it varies with respect to different offset level as well as moving direction, and makes system model much more complex.

Dynamic response

Dynamic response is always the most interested part in mechantronic system design. First, as shown in figure below, some beat could be obtained in time domain response when a sinusoidal signal is loaded to the system.

In general case, beats will never happen in such a simple input condition, because it's a result of combination of two wave with different frequency, once it happens, some kinds of harmony takes place inside the system. To locate this harmony, spectrogram analysis is done for the setup. Spectrogram is kind of frequency information plot that can indicates full magnitude and phase information of each specific frequency at each specific sample point [6]. Detail introduction to spectrogram is elaborated in appendix. Spectrogram of input to output is shown in figures below, for this analysis, sampling window is 1000 while sampling offset is 250, window function is chosen to be Hann window [7] [8].

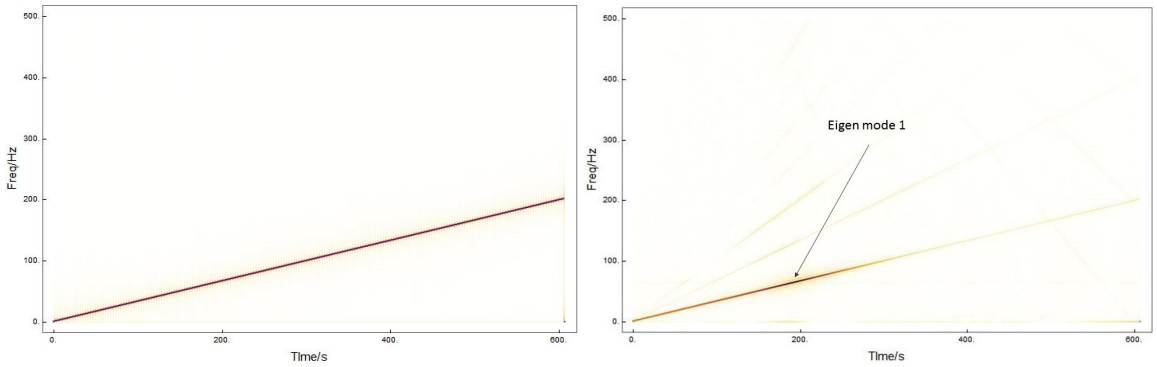

(a) Input signal (b) Output signal

Figure 4.6: Spectrograms of A15 identification test

slope of ramp lines in figure 4.6a indicates that the input signal is a sinusoidal wave whose frequency rises with time, however, figure 4.6b, which represents information of output signal shows more lines rather than a single ramp line. This phenomenon indicates that the system meets a harmony problem, and due to this harmony system behavior will become quite nonlinear even at a very low frequency range. detailed disturbance classification is listed in appendix.

Based on the identification test data and spectrogram study, the system is not a simple SISO system but a SIMO one, so it is not possible to make the exact bode plot of transfer function from input to output. However as shown in the spectrogram, the linear part of the relationship between input and output is the major one of linear and nonlinear relationship. Since we already know how other frequency affect the system, it becomes possible to linearize the relationship, that is, based on the input signal information, any frequency components that comes from system shortcuts can be filter out and the SIMO system is simplified as a normal SISO one. This method will also be used in following section to find the linearized transfer function.

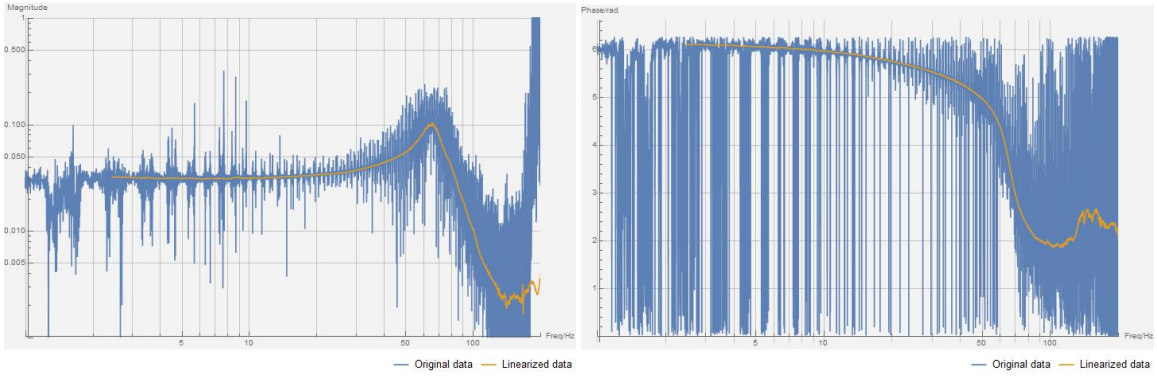

(a) Gain plot (b) Phase plot

Figure 4.7: Bode plot of A15 piezo bender

It is clear that due to harmony problems mentioned above, not like affects from other kinds of nonlinearity [9], even if at very low frequency range, the original data curve is rough and has lost of nodes while the linearized plot is much better, it's smooth and the important features of the original curve shape are maintained in the linearized one. According to this linearized bode plot, A15 piezo within testing frequency range is a third order system with eigen frequency at around $70Hz$ and a pole at around $80Hz$.

Hysteresis

To obtain hysteresis feature of this piezo, a slight changing sinusoidal signal is added to the setup and results are shown in figure**??**

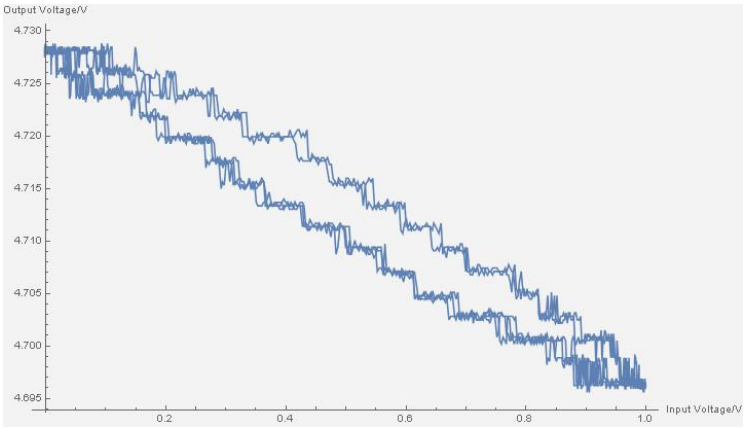

Figure 4.8: Hysteresis of A15 bender

The hysteresis loop is step curve rather than a smooth one, the reason is that resolution of the position sensor used in this test is not high enough, so the real smooth curve is discretized into this step form. According to the test result, A15 piezo is symmetric hysteresis device and can be easily controlled.

4.1.4. A12 piezo

Experimental process for A12 piezo are similar to that for A15. Analysis is also based on its static, dynamic and hysteresis features.

Static analysis
A12 piezo also meets a piezo release problem as shown in figure below and it is even more serious than that of A15 piezo. More than jumping to another state, it even goes back to some where behind the initial position.

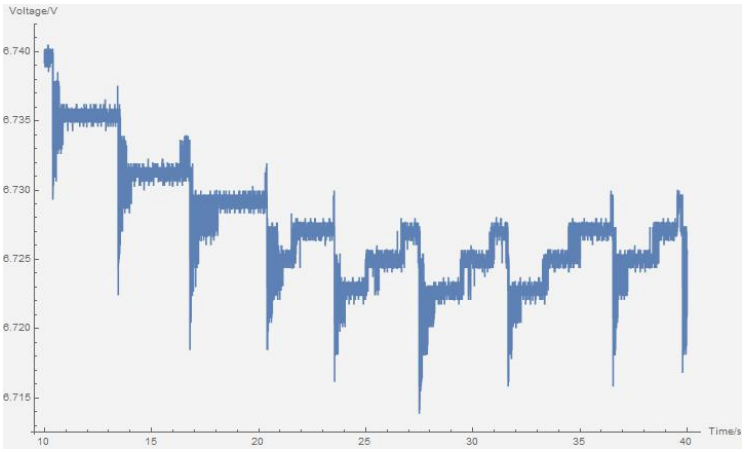

Figure 4.9: Piezo releasing phenomenon on A12 piezo

Dynamic analysis
Second, is about Dynamice response. spectrogram method is still used on A12 bender. Only gain spectrogram from input to output is shown in figure below, while spectrogram of original input and output signal are listed in appendix.

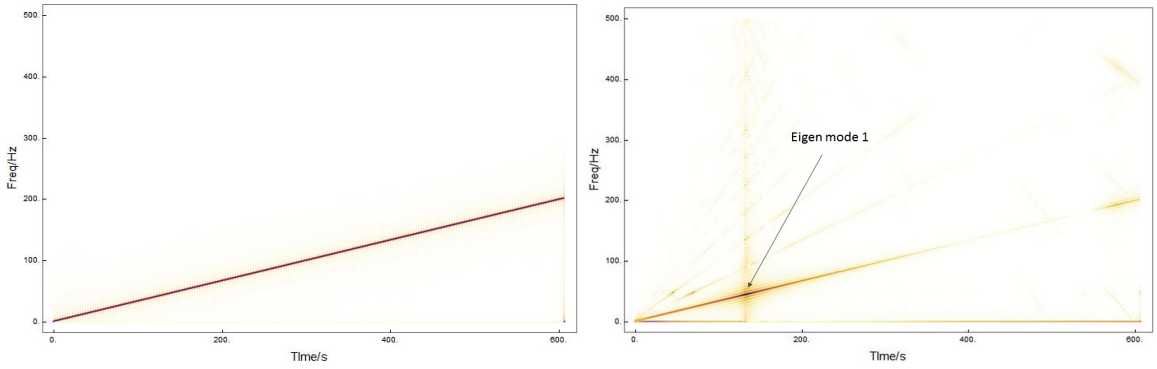

(a) Input signal (b) Output signal

Figure 4.10: Spectrogram analysis of A12 harmony

Comparing input and output spectrogram, A12 piezo shares the same response features with A15 piezo, this piezo has two eigen mode within the tested frequency range and meets a serious harmony problem.
Base on the identification data, the linearized and original bode plots of transfer function of A12 piezo bender from input to output is plotted and shown below.

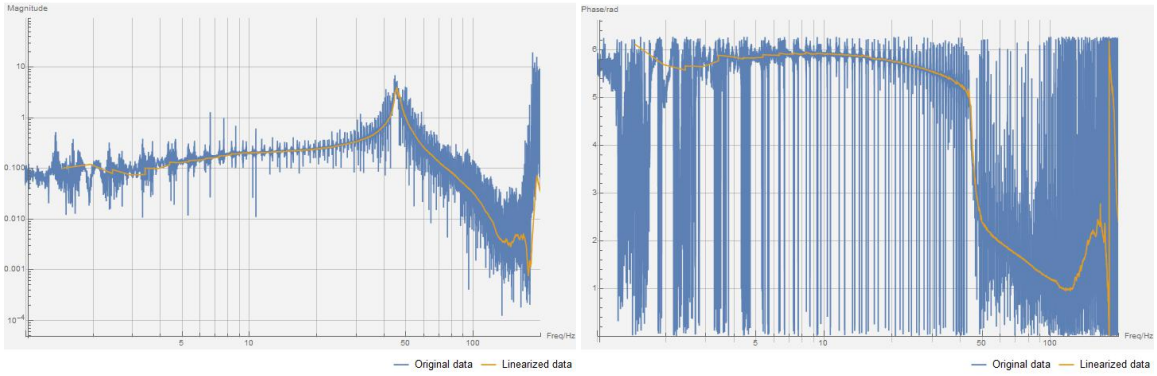

(a) Gain plot (b) Phase plot

Figure 4.11: Bode plot of A12 piezo

Results are similar with A15 piezo, original data based curve of bode plot is rough and blur, but still the linearized plot can indicate that A12 piezo bender is also a third order system with eigen frequency at around $45Hz$ and a pole at around $80Hz$. Besides, it is obvious that gain of A12 piezo is larger than that of A15 piezo, which means that A12 piezo bender has a better mobility.

Hysteresis
Result of hysteresis analysis for A12 are list below.

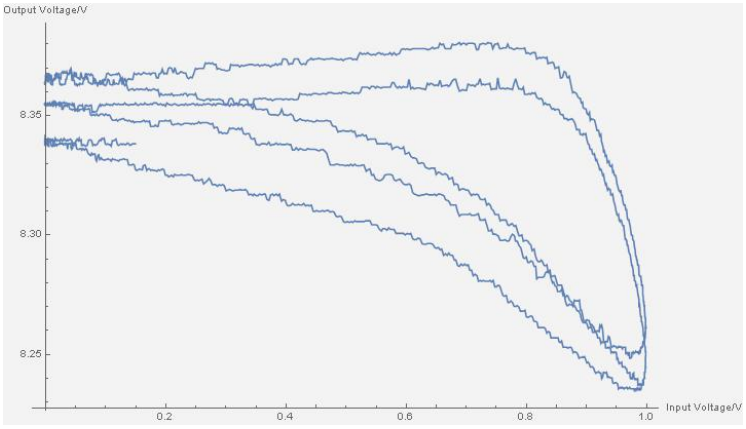

Figure 4.12: Hystersis loop of A12 piezo bender

According to the plot, first the response first goes up and then goes down when input is continuously rising, and straightly goese back when input descents. Hence hysteresis of A12 piezo becomes so abnormal, it is asymmetric and even not monotonous, which hugely increase the difficulty of controller design

4.1.5. Conclusion

It is easy to see and understand A12 and A15 piezo share almost the same kind of response feature and problem, because of the same piezo material used inside. Both of them are a second order system within test frequency range and affect by the harmony effect, grid disturbance and amplifier defects. However, all these problems are much more serious on A12 piezo bender.

Spectrogram clearly showing that both these two piezo benders are second order systems and also indicate that system features will be strongly affect by the three disturbance list above, these disturbances bring a huge set of parasitic frequency components to the system and forms a lot of virtual eigen modes. Although

real and virtual eigen modes are distinguishable in spectrogram, they are hardly seen in time domain response and really affect the time domain response. Input energy will not only be distributed and wasted on those virtual modes which leads to a lower efficient, but also add unnecessary vibration to the system.

Comparing the two piezo, it is obvious that A12 has an advantage of higher gain ans mobility, however it also has more shortcoming, first, this piezo meets more serious harmony, second it has a unfriendly hysteresis feature, Eventually and most importantly, eigen frequency of this piezo is relatively lower, which will limit overall performance of the complete system.

As a conclusion, even though the A15 piezo still has some disadvantages, it is much better than A12 piezo and becomes the choice of next experiment phase.

4.2. Complete hinge test

After identification process of available piezo bender, type A15 becomes the choice in next experiment phases. In this section, following the prototype design proposed in chapter 2, a complete compliance hinge with A15 piezo bender has been built and identified.

4.2.1. Introduction to test setup

Considering the test prototype should be compatible with equipments available, design proposed in previous chapter has been slightly modified to adapt to sensor resolution, mounting geometric and etc. Modified prototype is shown in figures below, detail dimension specs are listed in appendix. Modifications are concentrated on the length of beam and mounting maneuvers. To adapt relatively low sensor resolution, length of the beam is doubled to achieve a lager motion. Some groves are added on the base for wiring purpose.

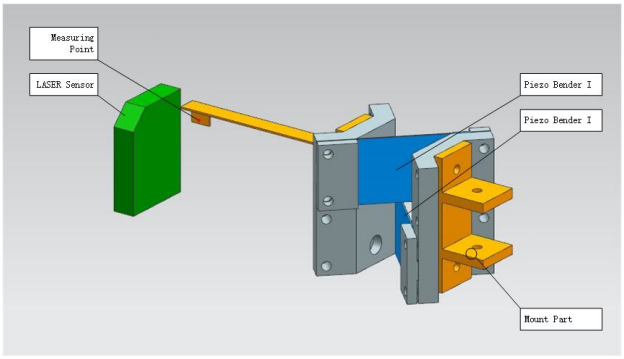

Figure 4.13: The completed test prototype in CAD design

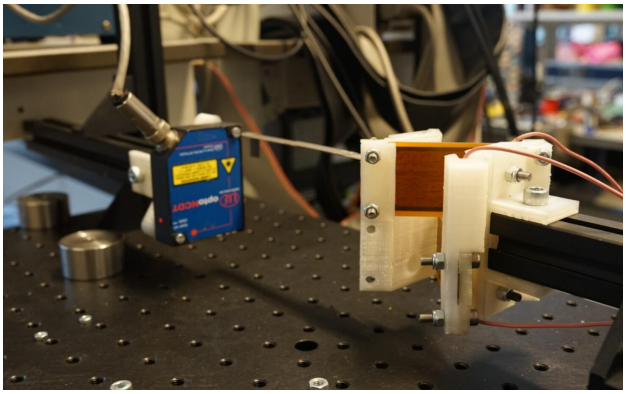

Figure 4.14: The completed test prototype

Those white parts are base components made with 3D printing technology, brown parts are A15 piezo

benders, gray part is steel beam and black parts are test platform made of aluminum profile.
circuit connections of this test prototype are shown in figure below.

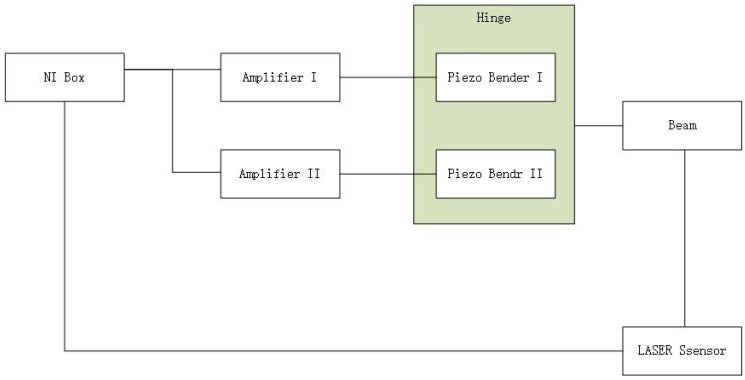

Figure 4.15: Device connection

Test signal is still generated by NI measurement box, however, in this section, this signal will be first duplicated into two identical signals before sent to two same-type amplifers. Then amplified signals will be loaded to the two independent piezo bender on the compliance hinge. Identification process is similar to what is done in piezo bender test. Both dynamic and stasitic response is studied [10].

4.2.2. Identification result

Dynamic response
In this section, identification in mostly about dynamic response, because this part matters a lot in controller design, while other parts like coming back, hysteresis could regarded as disturbance and been compensated later.

As ready studied in previous section, Piezo bender used in this project meets serious harmony effect, and this effect will continuous in the hinge test. Spectrogram of setup gain is shown in figure below, while spectrograms of original input and output signal are listed in appendix.

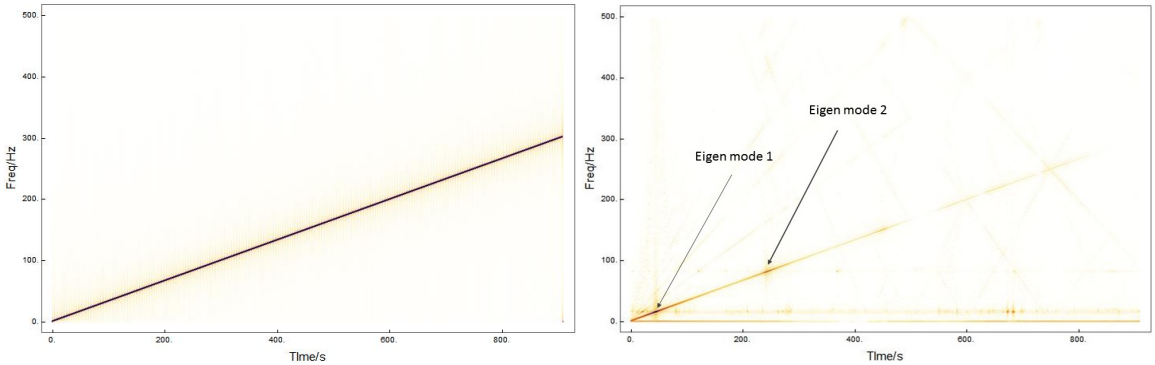

(a) Input signal (b) Output signal

Figure 4.16: Spectrograms of the complete system

As what's predicted. this complete hinge also meet a very serious harmony problem. Multiple frequency components appears in the output signal and deprave performance of whole system. So the overall bode plot of the system will be more rough compare with linearized bode plot, which are shown in figures below.

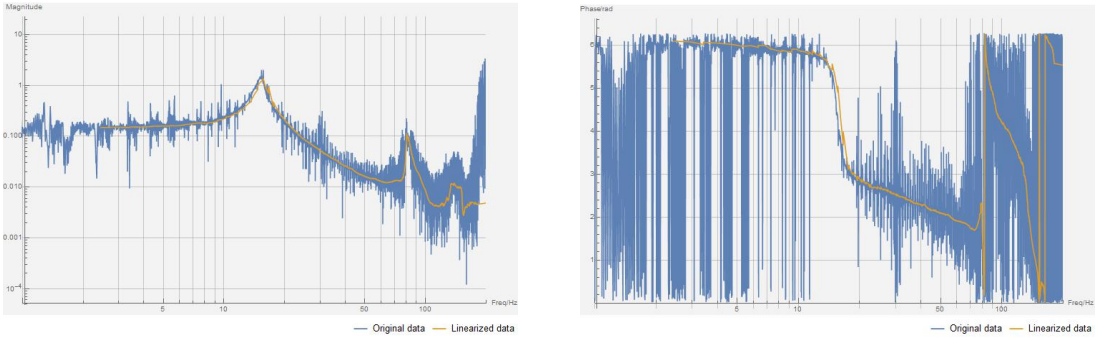

(a) Gain plot (b) Phase plot

Figure 4.17: Bode plot of system transfer function

According to the bode plots, the whole setup also suffers a lot from harmony effect, the curve of bode plot is still rough and with lots of vibration along the whole operation frequency range. The linearized curve is smooth and shows a feature of fifth order system with 2 resonance peaks at around $20Hz$ and $80Hz$ as well as a pole at around $30Hz$, which matches previous FEM analysis and identification of A15 piezo bender, one mechanical resonance peak at around $20Hz$, one electric resonance peak at around $80Hz$ and one pole. The rapidly dropping phase around the two eigen frequency indicates that damping ratio of both the two eigen modes are very low.

Hysteresis
Hysteresis analysis of the complete setup is shown below.

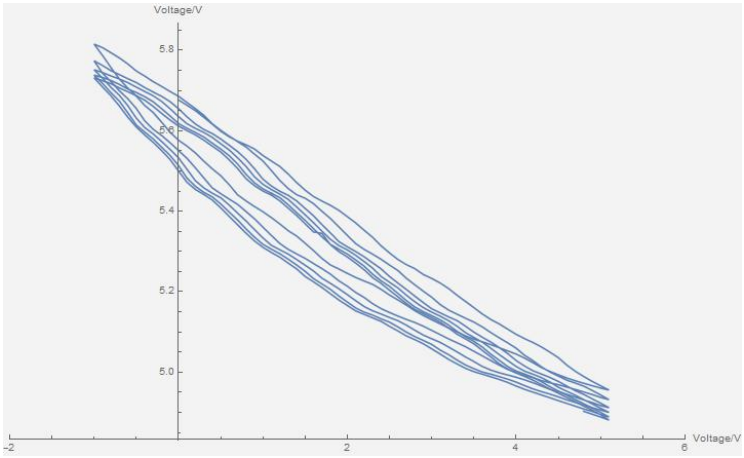

Figure 4.18: Gain plot

Figure 4.19: Hysteresis plot of the complete setup

Hysteresis plot of the complete setup is similar to that of A15 piezo shown in figure 4.18. It is because that the compliance mechanism do not introduce any new significant hysteresis source to setup, so all the hysteresis comes from the A15 piezo used in the setup. Like A15 piezo, hysteresis of the complete setup is gentle and symmetric.

4.2.3. Transfer function fitting

As inferred above, the setup is fourth order system with two peaks locate at around $20Hz$ and $80Hz$. To obtain the exact transfer function eigen frequency as well as other important parameters, date fitting is implemented for the linearized bode plot.

The to-be-fitter mode is formulated as a general fourth order system as shown in eq4.1

$$tf = \frac{n}{(s^2 + a * s + b)((s^2 + c * s + d)(s + e)} \tag{4.1}$$

where n,a,b,c,d,e are to be fitted parameters. Fitting results are list below

	Estimate	Standard Error	t-Statistic	P-Value
n	7.55×10^{10}	3.807×10^{6}	77.5	3.835×10^{-313}
a	6.94	0.1206	57.53	2.79×10^{-245}
b	10624	13.38	793.5	3.6×10^{-902}
c	22.72	2.024	11.22	1.17×10^{-26}
d	269659	1789.26	150.9	1.51×10^{-476}
e	254.9	30.03	8.48	1368×10^{-16}

Hence, the transfer function is fitted as eq4.2

$$tf = \frac{7.55 \times 10^{10}}{(s^2 + 6.94s + 10624)(s^2 + 22.72s + 26959)(s + 254.9)} \tag{4.2}$$

And bode plots of fitted and original data are listed below.

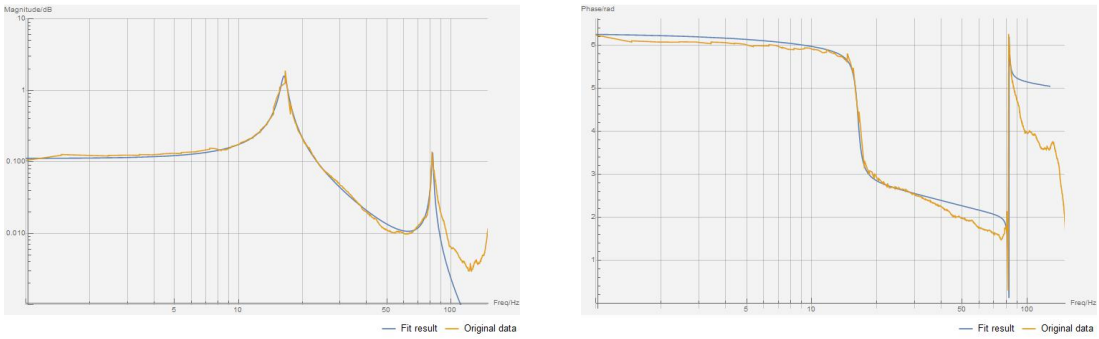

(a) Gain plot (b) Phase plot

Figure 4.20: Result of data fitting

According to these results, system model fits well only within $100Hz$ range. When frequency goes beyond $100Hz$, fitting error blooms up because of unconsidered high eigen modes. However considering two reasons, this fitting precision is already sufficient for controlling design [11]. First, these high order eigen modes only affect system behavior in high frequency range that is far beyond controlled bandwidth, Second, this fitting process is only based on the linearized model which fits well the real model only within $100Hz$ range, so it make few sense to spend time on achieving a low fitting error in high frequency range.

4.3. Conclusion

System identification on both individual piezo benders and the complete hinge prototype captured a rich amount of system model and potential problems. The fitted transfer model will be used in following controller design process and these potential problems such as nonlinearity and external disturbance will also be considered to ensure performance of the controlled system.

First,it is important to notice that the transfer function obtained in this chapter is only based on the linearized model,nether harmony nor external disturbance are include in this linearized model. So that the transfer function based controller design method can‘t well handle this setup if without extra effort. To ensure

controller reliability, extra attentions need to be paid on the error between nominal model and real system, in another word, more reductive becomes necessary to maintain stability and performance. However, more reductive will reduce system bandwidth at the same time, so an optimized balance point between robust and speed is necessary to guarantee overall performance.

Second, as seen in static analysis process, extra motion happens after the temporary steady state. Piezo bender will still move after staying at a steady state for a while. Due to this feature, this setup could be regarded as a combination of two individual model, one model makes the piezo bender move to first steady state, the other model force it moving from first steady state to the second one, and the second model can regarded as a disturbance.

Thirdly, due to hysteresis and non-linearity of piezo material, system shows different behavior at different offset level and different operation amplitude. And time domain identification method used in this project doesn‘t consider this type of variation, so that the transfer function obtained in previous section is only an average expression of all possible results. Hence, a feedback loop becomes very necessary in controller design to compensate the model error.

5

Controller design

5.1. Introduction To Real Time system

It is very fast and efficient to design and test control algorithm in simulation softwares like SIMULINK, however control algorithm needs to be implemented on real equipments in the end. To finish this step, a programmable hardware is needed to act as the bridge between real instruments and virtual algorithms.

Our daily using PC is a kind of devices who can easily handle thousand types of tasks, However control tasks are not include in these tasks. Because common computer systems are usually soft time based device, a soft-time device takes lots of operation steps before completing a single task, extra operation layers such as OS task manager, CPU task distributor will cut a simple task thread into several subtask slices and complete them in parallel or in series but in a random priority. These unforeseen randomness makes a lot of trouble when dealing with control tasks which require a very high time accuracy and restrict response speed. For a example, when a soft time controller is trying to handle a feedback algorithm, controlling machine can not even guarantee that a feedback algorithm is following the order of measuring, calculating and output.

Real time system is a type of hardware where programs can run at real time. Because of its unique logical architecture, real time device can guarantee that every program running at its desired priority, timing and speed. Due to this huge advantage, real time device appears appears in almost every single control system.

In this thesis, a real time controlling by dSpace is used as the control algorithm platform to apply the controller design to the prototype built in previous chapter,The Complete test prototype is connected as shown in figure below.

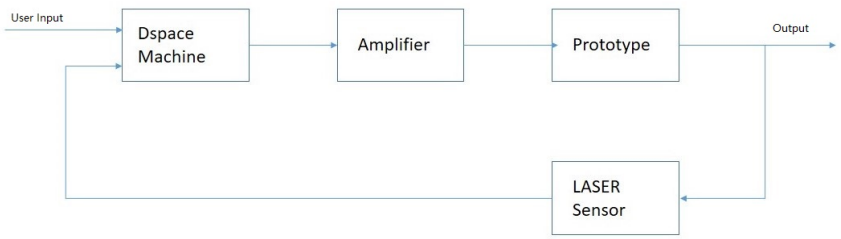

Figure 5.1: Setup structure

Because the position sensor used in this setup runs at 1000, processing speed of the real-time platform is also fixed at $1000Hz$. With the help of this real time machine and its control plane software, control maneuverer can be simply implemented on the prototype. First build control model in simulink, then compile this model into C code, finally load this code to dSpace machine and run it.

5.2. Plant review

Before design the controller, first, take a look a of the bode plot of the plant, which are shown in figure 5.2.

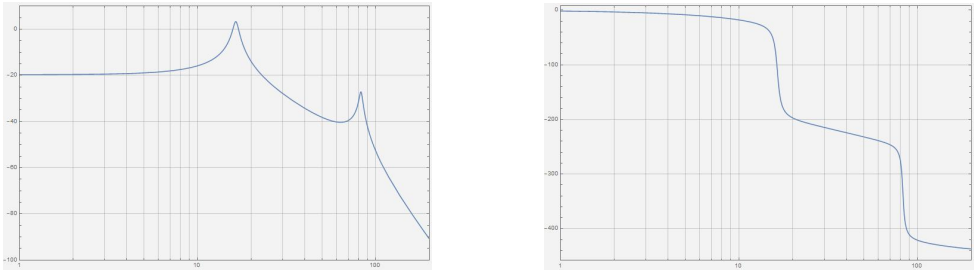

(a) Magnitude (b) Phase

Figure 5.2: Bode plot of the plant

Notice that this there are two peaks ar around $18Hz$ and $80Hz$, Considering that the system do not need to be at very high speed, it would be handy and efficient to set bandwidth goal to be around $25Hz$.

To achieve that goal, in this chapter, a controller for the test prototype has been built and tested, This controller is designed based on the linearized model identified in last chapter, the controller structure is mainly formed with three main part, feedfoward, feed back and a disturbance observer, schematic of this control architecture is shown in figure below and detail information of each part will be discussed in next sections.

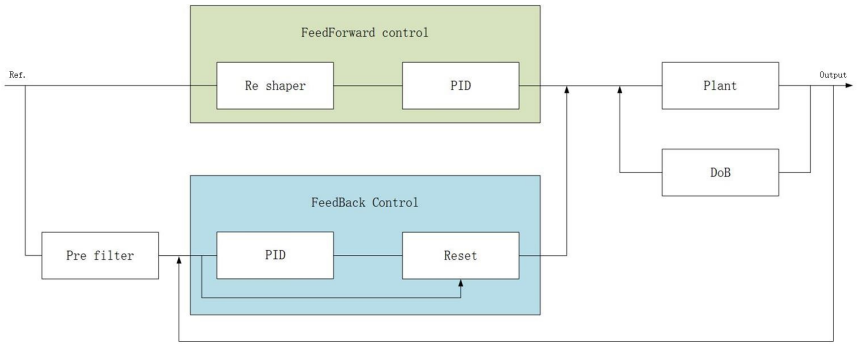

Figure 5.3: Controller structure

5.3. Feedforward control

Although the setup is quite non-linear, the basic linear model is not such a complex one, considering this advantage, a feed forward control method is doable in these case and can would be capable to greatly improve system performance. A typical system with feed forward is shown in figure

5.3.1. Inverse model PID

Inverse model feed forward controller is one of the best way to achieve a high speed control system in theory, however, in reality, it is impossible to measure the exact system model and get it inverse, anyway some kinds of error, bias will happen and limit the performance of feed forward control. Thanks to the feed back control

loop, even though there is some inevitable model bias in the feed forward loop, the final output can be correct by the feed back loop, and the feed forward loop can still increase system performance.

Considering that in Feedback design, system bandwidth is configured at around $27Hz$, between the two peaks, it would be handy to only get system model before $27Hz$ inversed, based on this idea, the feed forward controller should have a form of as shown in equation below.

$$tfunc = \frac{s^2 + 6.9s + 11945}{(s^2 + 300s + 360000)(s + 600)} \tag{5.1}$$

A second order transfer function which is the inverse of the first eigen mode of identified system model at numerator, and a third order low-pass with kick in frequency at $100Hz$ to make this feed forward proper.

5.3.2. Re-shaper

Just as what mentioned in previous section, this system meets s serious overshot problem when dealing with step response. Theoretically speaking this overshot can be compensated by a well tunned feed forward control, but in reality, it is impossible to build a perfect feed forward model, especially in such a non-linear case.

If only dealing with a step input some other method could be more efficient to significantly reduce overshot, that is, a step reshaper. A reshaper can divide a single step into several smaller steps and give them to the system in series with some time gap between each step. By well tunning step size of these sub-steps as well as step gaps, system's response to each sub-step will not be in phase but with some phase delay, which means vibration caused by each small steps will cancel each other, and increase settle down speed.

In this case, to achieve the best performance and stability, a ZVDD reshaper which will divide a single step input into 3 sub-steps, is applied. Amplitude and time delay are set based on following equation, where A_i represents amplitude of respect substep, t_i represent time gap between each substeps [12].

$$\begin{bmatrix} A_i \\ t_i \end{bmatrix} = \begin{bmatrix} \frac{1}{(1+K)^3} & \frac{3K}{(1+K)^3} & \frac{3K^2}{(1+K)^3} & \frac{K^3}{(1+K)^3} \\ 0 & \frac{\pi}{\omega_d} & \frac{2\pi}{\omega_d} & \frac{3\pi}{\omega_d} \end{bmatrix} \tag{5.2}$$

where,

$$K = e^{-\frac{\zeta\pi}{\sqrt{1-\zeta^2}}}$$

$$\omega_d = \omega_0\sqrt{1-\zeta^2}$$

Based on identification result, the first eigen mode of this test prototype matters most in system performance and eigen frequency of the mode is $18Hz$, damping ratio is about 0.07, so K is set to while ω_d is set to 102, a reshaped step signal example is shown below in figure below.

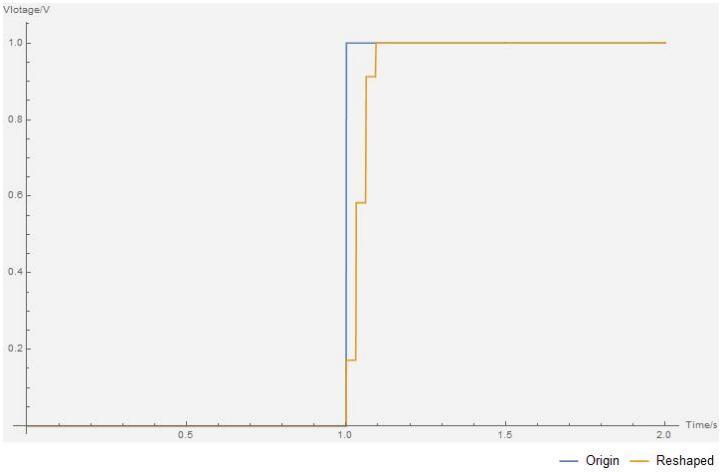

Figure 5.4: TA example of the effect of ZVDD reshaper

To test the effect of re-shaper, a square wave signal is applied. system response with/without this filter is shown in figure below.

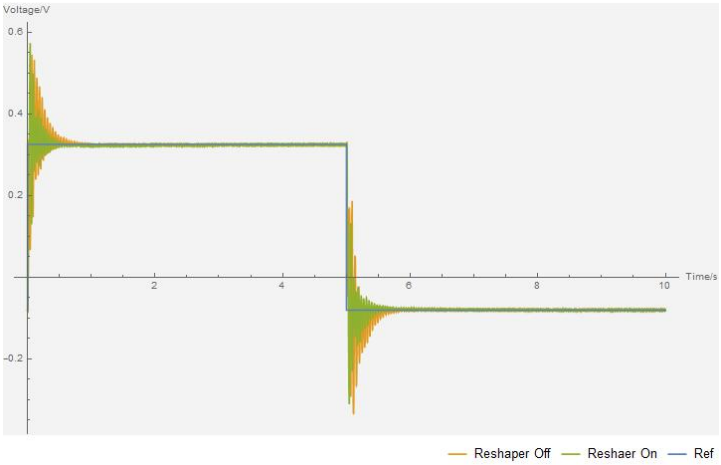

Figure 5.5: Test result of reshaper controller

Comparing these two curve, the re shaper successfully reduced settle time with step input. However, overshot changes little, it could be the result of imperfectness of the reshaper parameters, since the controller design is based on the approximate linearized mode rather than the real one, so that phase of each substep can not be able to have an exactly 180° interval and system gain at different offset level, in this case at different substep is quite different. As a result, over all performance of a re shaper is limited.

5.4. Feedback control

Feed back control can measure the output of a system, compare it with the reference signal, and adjust the output based on the input/output difference. A typical feedback structure is shown in figure below. This method is versatile and efficient in design process, but can cause some delay and may give some instability.

5.4.1. FeedBack PID

To achieve the bandwidth of $25Hz$, a proportional filter is firstly used to rise the gain line, considering that plant gain at $25Hz$ is around $-12dB$, to rise this point to $0dB$, a proportional filter with gain of 15 is implemented.

After implementing this proportional filer, a lead/lad filter is then used to rise phase of the system. Considering that BW of the system is at around $23Hz$, pole and zero of this filter are set to be at $5Hz$ and $30Hz$respectively.

Considering that the second bad damped peak will go across the $0dB$ line, a notch filter is used to flatten this peak this peak to insure the stability, pole of this notch filter is set to be at $100Hz$ while zero is set to $80Hz$, damping ratio for the zero is 0.1 while for the pole is 0.6 [13].

Damping ratio of the first peak is also low, so anti-notch filter with pole at $10Hz$,zero at $16.5Hz$ is implemented to rise phase after the first peak, damping ratio for the zero is 0.1 while for the pole is 0.5

Finally, an integrator with pole at $2Hz$ is applied to reduce steady state error.

After implementing all this filter, bode plots of open-loop transfer function is shown in figures below.

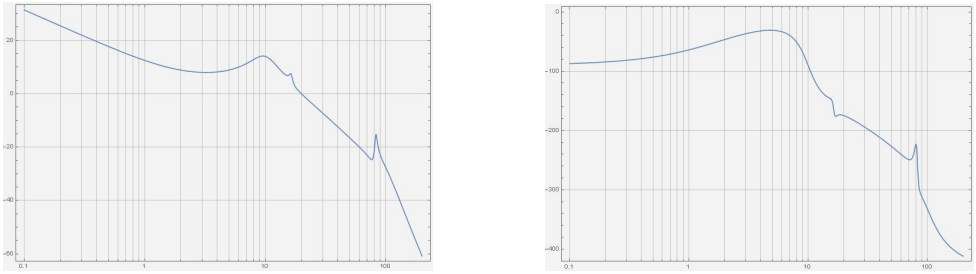

(a) Magnitude (b) Phase

Figure 5.6: Bode plot of open loop transfer function

With this controller configuration, system bandwidth is at $24Hz$ with phase margin of 8°. however, it is important to notice that there is a small gain drop at around $4Hz$ in open loop transfer function and its valley is already very close to $0dB$, this feature will decrease in bandwidth of the system in real practice and slow down the system, a pre-filter is needed to compensate this valley. Besides, it is also important to keep in mind that this controller design is based on the linearized transfer function, and according to previous study, the linearized transfer function is only a approximation of the real model, so all this parameters needs further adjustment when implemented to the real setup test.

5.4.2. Reset controller

Reset control is method that can rest the output or a sub state of a controller to zero when its input is zero. In most under damped system, it takes controller a lot of time to get the system settled down, because a feed back system always as some phase lag, hence there is always some extra unnecessary energy feed to the system. And this energy will force the system moving, in most case, vibrating, if under damped, it will take a lot of time for the system to attenuate these energy. But with the help of reset control method, the system can reduce unnecessary energy feeding. As a result, though the system is still bad with attenuate energy, the energy it needs to attenuate is much lower. Hence, settle down becomes much faster. Besides, since unnecessary energy feeding to system is lower, stability of the system can also improved [14].

In this case, since the system meets a lot unwilling high frequency vibration, the reset controller is deployed to reset high frequency component of controller output More specifically, the reset controller is connected to $5Hz$ high-pass filtered feedback controller output, and is trigger by the difference between reference signal and setup output, trigger tolerance is set $to 0.005V$. Output of reset controller is then summed up with the output of a $5Hz$ low-pass filter and finally send to the plant [15]. Structure of this reset controller is shown in figure 5.7 below.

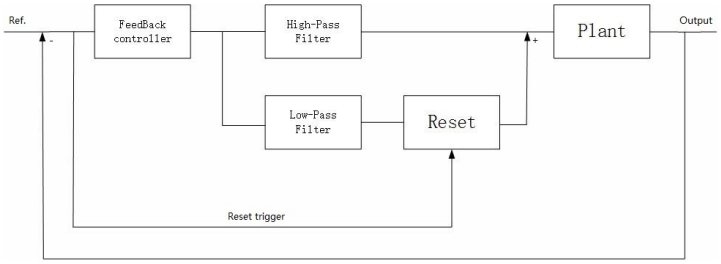

Figure 5.7: Structure of the reset controller

So this reset controller will only involved at the sharp point of reference signal. Test results are shown below. Those vibration at steady state are due to a sensor problem.

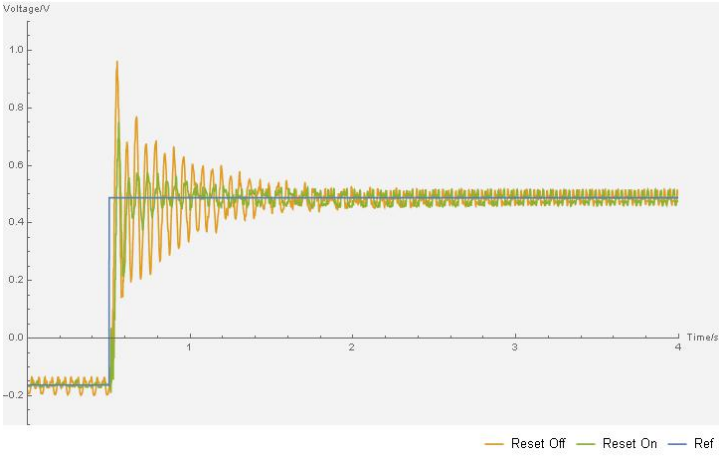

Figure 5.8: Test result of reset controller

According to the experimental data, reset controller significantly reduce settled down time when the the beam is moving to left, however, when it comes back to the right, effeteness of reset controller is almost zero. The reason could be system variation at different offset level, when the beam is going to the right, it goes to a higher offset level and with a better signal-noise ratio, so the reset controller can easily handle this case. But, when th beam is approaching to the left, offset level as well as signal-noise level goes lower, system features change a lot, and the $5Hz$ edging frequency is no longer a good choice. To achieve a comprehensive effect, the reset controller should be able to work at hybrid mode to meet different requirement at different working environments.

5.4.3. Pre filter

As mentioned in previous section, a gain drop at around $10Hz$ needs to be compensated, also considering that there is a small peak at $12Hz$, the pre-fiter is configured as notch filter, with zero at $6Hz$ pole at $20Hz$, damping ratio for zero is 0.9 for pole is 0.25. After implementing this pre-filter, gain drop has been risen for a little as shown in figure. however the cross over frequency is also reduced.

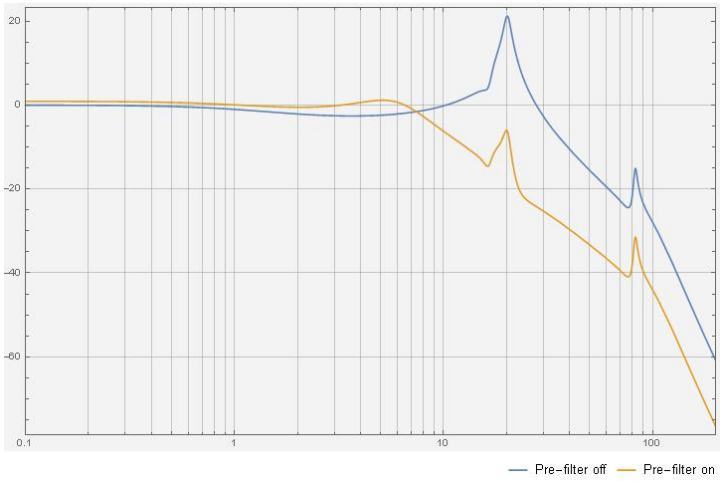

Figure 5.9: Bode plot of pre-filtered system

To test the effect of the pre-filter, a step test signal is applied to the system, response is shown in figure 5.10.

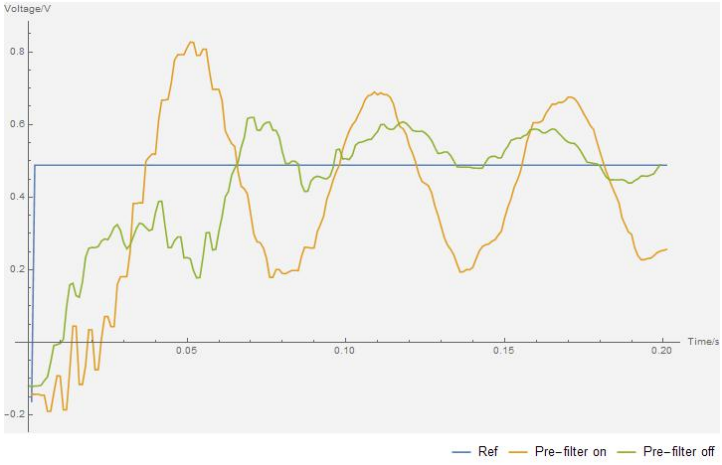

Figure 5.10: Test result of pre-filter

According to the test results, before implementing this pre-filter, it took the system two steps before reaching steady state because of the gain drop at around $10Hz$,. After applying this pre-filter, system behavior becomes smoother, however this pre-filter also introduce a disadvantage, that is, system speed goes lower.

5.5. Disturbance Observer

In previous identification chapter, it is assent that the model is an average approximation of a non-linear model, even though a controller could handle the approximation error, other effort is still available to keep improving the system. In this case because the controller is based on a nominal model, by regarding the error as a kind of disturbance, a disturbance observer could be implemented in the system to reject these disturbance, in another word, to reduce the error between nominal model and real model, and then improve performance.
A disturbance observer is a control maneuver that looks like a feed back method, instead of compare the the output and reference signal, it compare the real model and nominal model, and use a feed back signal to compensate the difference. A typical disturbance observer is shown in figure below [16].

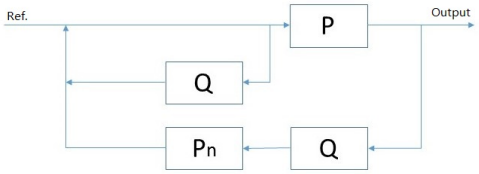

Figure 5.11: DoB structure used in this project

where block P represents the plant, block P_n represents the DoB expression, Q represents a low pass filter.

5.5.1. Disturbance review

Two model errors are considered as disturbance in this section.

Variable gain First is the different gain, piezo is a kind of very non-linear material and as anticipated in previous section, this setup shows very different gain at different voltage range.

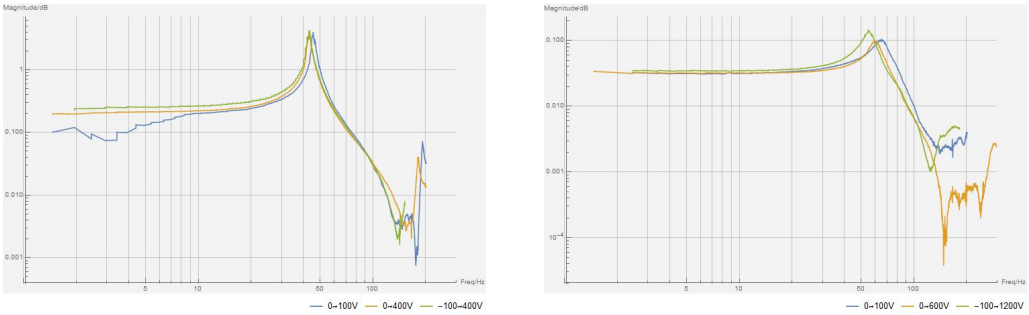

(a) A12 Bender (b) A15 Bender

Figure 5.12: Different response at different voltage level

Affect of this problem is shown below, where a sinusoidal signal is used as input signal, responses of two type of controller are plotted, one is the normal controller designed in previous section, another is a similar controller but without integrator, which can compensate steady state error.

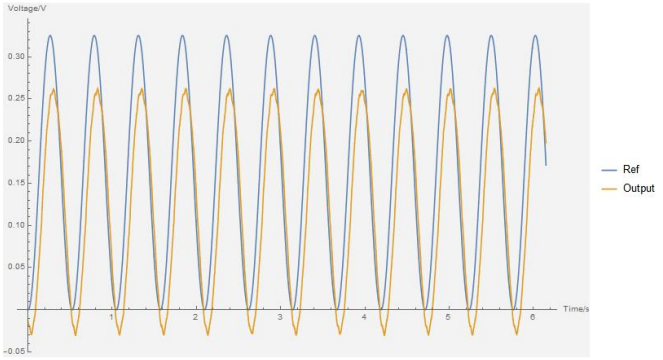

Figure 5.13: System Response without steady state control

According to these plots, the system is over driven at low offset level, while under driven in high offset level. It is because that system gain is different at different voltage levels, but the controller is only based on the mean value of all the possible gains, so when at low offset level, where the real gain is higher than the mean value, the system is over driven, and at high offset, where the gain is lower than mean value the system is under driven. It can be easily figured out that if without calibration, a model error can result in a huge output error.

Piezo releasing Second is the coming back phenomenon, as identified in previous chapter, it mainly happens in steady state, so a step signal is used to check the phenomenon, results are shown in figure.

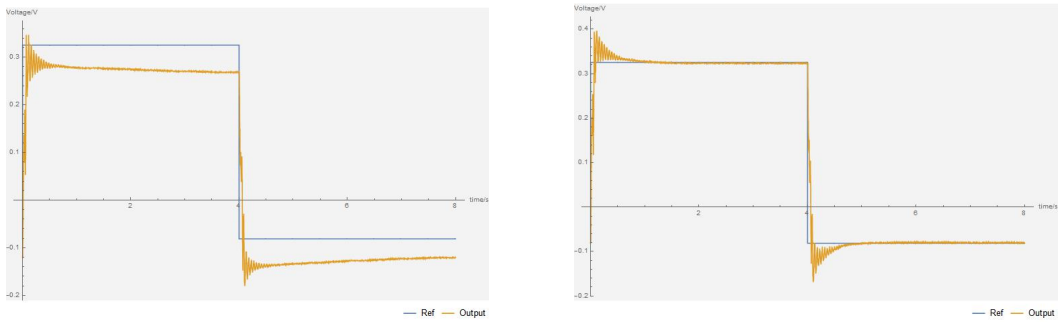

(a) System Response without steady state control (b) System Response without integrator

Figure 5.14: System response with step input

It is clear that after reaching the steady state, if without any steady state control maneuver, output will fall down back to neutral position, besides, affect of unfixed gain also present in step response. According to figure 5.14b. Even with an integrator, a feed back steady state controller, there is still a very small steady state error and this error is always at one side of reference signal.

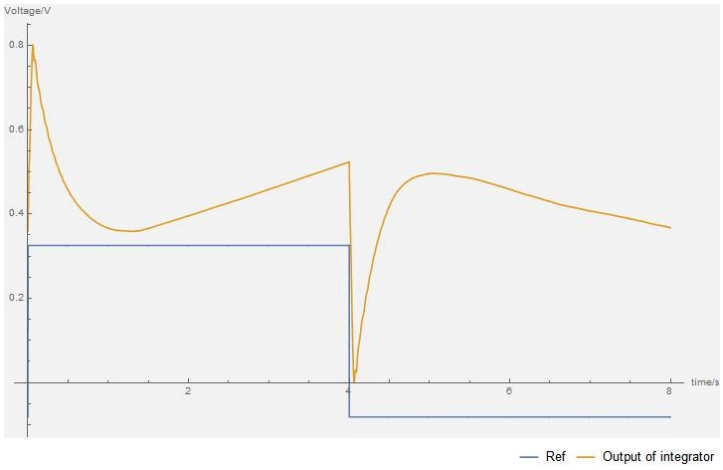

Figure 5.15: Control effort of integrator

What's more is that the output of integrator is continuously rising as shown in figure 5.15 , the rising orange line shows that piezo coming back is a continuous motion and needs to be actively compensated all the time. It is difficult to formulate the math model of coming back motion from the origin of this phenomenon, however if simplify it from results, it can be regarded as simple as a gain that also varies with time.

Eventually, these two different disturbances are concluded a special gain problem, which related to both signal voltage offset and time.

5.5.2. DoB design

Considering these two features and system bandwidth, the gain problem mainly matters in low frequency range, so the P_n should be the low frequency part of inversed nominal model at low frequency range [17], that is

$$P_n = 9.5 \tag{5.3}$$

and the low pass filter Q should kick in at low frequency, in this case, a first order low-pass filter at around $5Hz$ is implemented, so

$$Q = \frac{30}{s+30} \tag{5.4}$$

5.6. Finalized controller performance

After applying this disturbance observer, the complete system is tested by multiple types of signals, results of system with/without DoB are list below.

.

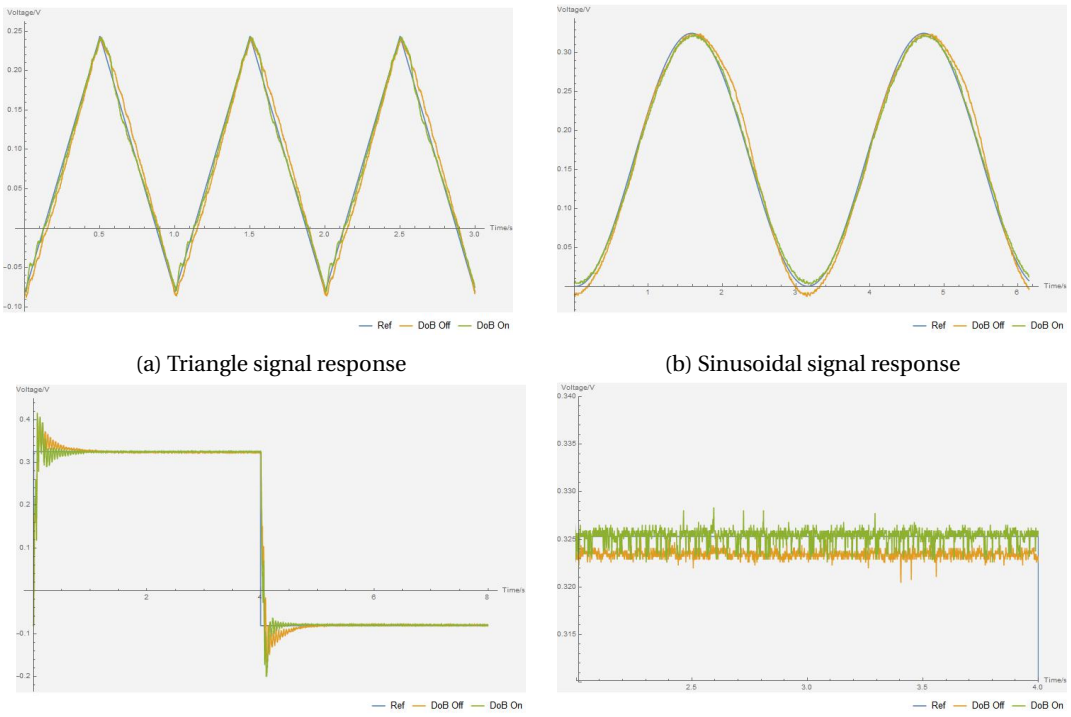

(a) Triangle signal response

(b) Sinusoidal signal response

(c) Step signal response

(d) A zoom in view of step signal response

Figure 5.16: System response under different input signals

These experiments show the great benefit of disturbance observer when dealing with model error at low frequency range.

Figure 5.16a shows results when dealing with a triangle wave, which contains both low and high frequency components. Although this DoB concentrates on low frequency parts, it still shows very nice performance in such a complex working condition, because in most trajectory tracking task, low frequency parts govern the route shape most. Once these parts are well controlled, the system can make a very nice tracking result.

Figure 5.16b shows the effect of DoB when dealing with a signal which is exactly at the target frequency range of DoB. At this condition, DoB can not only compensate most over shot at peaks but also significantly reduce response delay companying with feed forward control.

Figure 5.16c and 5.16d mainly show the effect of DoB at steady state, according to these two figures, it is clear that steady state error has been well attenuated. And these following statistic data gives a numerical analysis results.

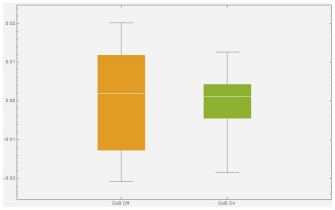

Figure 5.17: Error distribution of step response

Triangle Wave

Parameters	DoB Off	DoB On	Improvement
Median	0.00197	0.00115	41.6%
50% interval	0.0245	0.00879	64%

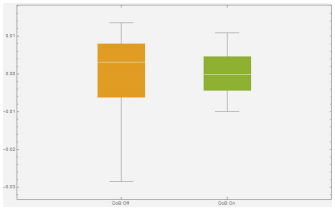

Figure 5.18: Error distribution of sinusoidal response

Sin Wave

Parameters	DoB Off	DoB On	Improvement
Median	0.00301	0.000171	43%
50% interval	0.014	0.00904	35%

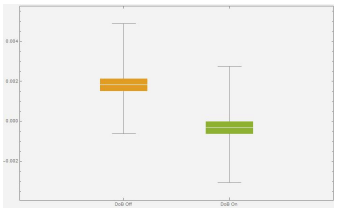

Figure 5.19: Steady state error distribution of step response

Step Wave

Parameters	DoB Off	DoB On	Improvement
Median	0.00182	-0.000301	64%
50% interval	0.00061	0.00609	0.16%

Based on the statistic results, disturbance observer greatly improved response accuracy and precision at the same time when compensating offset depended variable gain, in these experiment, system performance is improved by at least 35%. As for steady state error, which results from piezo releasing phenomenon, this DoB can only improve accuracy, in this case, by 64%. Besides, DoB also reduces load of integrator as shown in figure 5.20

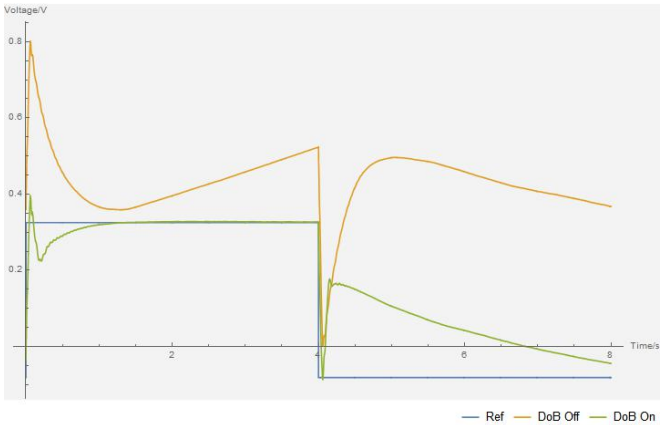

Figure 5.20: Output of integrator

according to the results, loads on integrator is also greatly reduced.

According to test on the prototype, although limited by the deflection range, mobility of a piezo compliant hinge is not at the same level of a conventional pin joint, it can still move around a relatively wide range and maintain high precision at the same time.

With multiple control technologies, the finalized controller makes this prototype reach a bandwidth of about $23Hz$, which already meets the design goal, even thought the system so non-linear that a single bandwidth can not guarantee the performance, with help of other control algorithm such a DoB, nonlinearity is well attenuated and the final performance is proved to be good enough to be used in positioning purpose.

6 Conclusion

Piezo-flexure hinge shows nice performance according to this study, however, negative results always come with positive ones. For advantages, this hybrid hinge design can achieve a very high moving precision and moving speed at low weight and size level. For disadvantages, due to the limit of piezo material, mobility of this design is not high enough to meet requirements from every manipulator, besides, even if to achieve such a low moving range, piezo ceramic requires a very high operation voltage.

Although these disadvantages are non-negligible, these unique advantages can still ensure a promising application in practice. Considering the two side of piezo-flexure hinge, it may not be able to take the place of every pin joint of a machine because of its low mobility, but it can still well handle some special cases where the moving range is not at the first priority or it can be implemented in hybrid configuration that use both conventional pin joint with on-joint actuation and piezo-flexure joint at the same time on a same machine to take advantages of both the two design and reduce their shortcuts. For examples, piezo-flexure hinge could be used in high precision multi-stage positioning system, where the required moving range is usually low. Or it could be used only in some stages of a manipulator, as mentioned in previous chapter far end stages are most sensitive to weight, so these kind of piezo-compliance hinge could be implemented in that part to achieve a precision goal at a low weight cost, and still use conventional pin joints at stages that are close to the base, so, due to the chain reaction, total performance of this manipulator could be improved when the mobility are still maintained.

6.1. Achievements

Hinge design Considering that there are hundreds of possible piezo-compliance hinge desgin. Two types of basic hinge configuration are studied in this thesis .
First, compliance mechanism itself is a good choice in a weight sensitive environment, in this case, an arm type manipulator. Because a compliance mechanism takes advantage of deflection of metal flexure, only some thin plates can achieve all requirements of a hinge. Hence, conventional heavy and bulky parts such as bearing, shaft are no longer necessary in a compliance mechanism and lots of weight budget could be saved and be reused in other places such as a better sensor or a larger payload. what‘s more, in precision working environment, due to its unique working principle, compare with pin joint, compliance joint will not meet gear tolerance problem, every single force input will directly result in a angular motion and makes it a better choice in high precision tasks.

Second, piezo ceramic is a very good type of piezoelectric material to be implemented in piezo compliance hinge for its metal-like mechanical property. Thanks to this advantage, it becomes possible to build compliance hinge directly with piezo bender, instead of using metal-piezo-stacked flexure, or even use a hybrid configuration that use both piezo and metal flexure at the same time. This simplification makes the whole design even more compact and lighter weight.

Third, combing compliance flexure and piezo bender gives more flexibility in hinge design, to achieve a

desired mobility, solutions could be modifying flexure configuration to achieve a desired stiffness, or modify ratio of piezo to metal flexure to achieve a desired force output, more flexibility helps this type of hinge be able to meet different working environments that have different balance points among weight, mobility and precision.

Prototype building and validation A positioning system can not survive without control system, to validate this design in practice. A prototype of piezo compliance hinge has been built and further experiments has been done to check its dynamic features as well as verify controllability.

Considering imperfectness of every singel piezo piece or over constrain of compliance mechanism, are not conclude in simulation. A test setup has been built to check and locate considerable unique features of a piezo compliance hinge, following system identification and controller design are based on this test setup.

According to system identification, some key features that will affect controller performance have been located.

First, A butter fly compliance hinge usually has its first eigen mode at relatively very low frequency, while others starts at a relatively high frequency range, however in a piezo comliance hinge, influence of piezoelectric is never ignorable. In this case, one important feature is that coupling between piezo and amplifier results in a electric resonance at around $80Hz$, same scale as the first, mechanical, eigen mode. So that, when dealing with a piezo compliance hinge, at least one more eigen mode needs to considered compare with a normal compliance hinge. Considering that the high precision stage do not need to be at very high speed, so working bandwidth is not necessary to be very high, that is, only two eigen modes matter in this case and the test system could be regarded as a fourth order.

Second, not like other common electric device, piezo material is capacitive rather than inductive, which results in a harmony problem. Due to this harmony, spectrum of the input signal will be widely expanded, for instance, a $10Hz$ sinusoidal wave will be expanded to a signal which contains $10Hz$, $20Hz$,$30Hz$ and so on frequency components. Hence, apparent eigen modes will be significantly increased and as a result, controllability as well as performance of the piezo compliance hinge will be reduced.

Third, the offset-depended gain, another important feature of piezo material. Due to the affect of this phenomenon, system gain at different voltage offset level is different, that is, at high voltage offset, system gain is lower than that at low voltage offset. What‘s worse, a normal time domain system identification, which is used in this thesis, can only find the average value of all possible gains. So if a controller is designed based on the identified model, its performance can‘t be guaranteed without compensation. Model error will result in a lot of problem such as, lower stability, significant response bias.

Fourth, the coming back phenomenon, which will mainly affect steady state response. It is a very typical feature of piezoelectric material, when applying a certain voltage, piezo will first move to position I, and then after a while, will slowly go back to position II. What‘s even worse, distance between Positon I and II is not a constant, but another offset voltage depended value. Because of this phenomenon, time domain identified system model only matches transient state, if a piezo compliance hinge goes to steady state, error between real model and identified model will become larger and larger and finally resulting a significant steady state error.

In this thesis the control task becomes handling a fourth order system with strong model uncertainty and still maintaining high preicison and increasing response speed as high as possible. To control such a system with an approximate model, or in another word, a model with partially known uncertainty, a design process is then proposed. The basic idea of this precess is first control the nominal mode, second is to reject model error, third is reduce system vibration and improve performance.

To control the system, desired bandwidth goal is set to be at $25Hz$, first a basic controller frame has been built based on the linearized system model, in this model all model imperfectness such as hysteresis, harmony are not included. For the feed back control loop, a PID controller has been implemented to tune open

loop transfer function, mainly dedicated to raise system phase and notch the second peak to ensure performance and stability. Considering model imperfectness and relatively low first eigen frequency, a feed forward loop which is based on the inversed system model is added to reduce working load of feedback and maintain working performance at the same time.

Both the two control loops are all based on approximate model, to make the controller practicable, further improvements are proposed. In this thesis, the coming back phenomenon is considered as a gain varying at very low frequency, hence, coming back phenomenon and offset-depended gain can be regarded as a same type of model imperfectness, a disturbance observer is implemented to compensate this kind error, this observer is configured working at low frequency range and trying to make the system following the nominal low frequency gain. This type disturbance observer resulting a system model that is more close to the nominal model used in controller design, in another word, practicality of the controller is ensured. Besides, performance of feed forward control is highly depended on the accuracy of system model. with calibration of disturbance observer, feed forward performance is further enhanced.

Some other algorithms are then applied to enhance over all performance. Because in reality, harmony do reduce the feasible bandwidth, as a result the complimentary sensitive gain around $10Hz$ drops a little and slow down system speed, a pre-filter is applied to compensate the drop. A step reshaper is then implemented to reduce settle time as well as vibration when dealing with step response. Stability of the system is also lower in reality, to reduce non-necessary energy input and improve performance, a reset controller is also used to reduce vibration.

By combing these efforts together a comprehensive controller has been built, problems such as response error caused by model imperfectness, vibration caused by harmony are compensated, test setup shows good result when dealing with positioning task.

As a conclusion of all works done in this thesis, conflict between high precision and high mobility can be simplified as conflict about weight, to solve it, piezo compliance hinge, a very compact and light weight design is proposed, and shows nice performance in both simulations and real world prototype tests.

6.2. Recommendations

Although the test prototype shows a very nice performance, there are still a lot of work could be done to further enhance the performance and achieve a facile and powerful mechanism structure at the final end.

First is that system harmony can be solved from its origin, a better performance amplifier could be used in future research, although affect of harmony can solved with non-linear control algorithm such as reset control, solutions that based on problem‘s origin are always faster and robuster. Also other types of material are also worthy trying, piezo material is powerful and featured with nice mechanical properties, however, it requires relatively very high driving voltage, which makes it not suitable in some filed such as on-body equipment of electromagnetic sensitive environment.

Hybrid configuration is promising, a more complex structure with different combination of different piezo and other material could give higher possibility and potential to achieve a better performance. However in this thesis, only one configuration has been tested, if possible, further experiments could focus on a more complex structure. Using customized piezo bender to achieve a special shape of hinge shape or combing different types of piezo in one single hinge to achieve special output feature, are very worthy trying. Besides, design in this thesis is not the optimal, a configuration with both piezo-flexure and metal flexure should also be high valued in further design and study. Because it gives more DoF on tuning hinge performance and mobility to reach a wider moving range and higher performance than the basic design proposed in this thesis.

Active compensating for piezo problem is another working direction. In this thesis, disturbance observer is used to compensate model error caused by piezoelectricity, however, this method is kind of feedback type compensation, a more precise and accurate modeling process could make it possible to have a high performance feed forward type active compensator to have a better compensation, higher speed and higher working range.

A

Introduction to spectrogram

Spectrogram is visual represent of spectrum of a time series data. Working principle of making a spectrogram is first sampling a time series data with fixed windows width and window offset, then using DFT method to obtain spectrum of each sample, compressing the 2-D curve to a 1-D line by using color depth to represent amplitude and finally put these lines together following sampling order. So that for a spectrogram, x-axes represent sampling series, y-axes represents frequency and color depth of point at (x_1, y_1) represents Amplitude of frequency x_1 of sample y_1.

There is a brief example to show how spectrogram works, assume there is a signal built with following expression, a combination of a sinusoidal wave with constant frequency of $100 rad/s$ and another sinusoidal wave with variable frequency starting at $200 rad/s$, rising by $20 rad/s^2$

$$y = Sin(600t) + Sin((200 + 20t)t) \tag{A.1}$$

Spectrogram of this given signal is shown in figure below

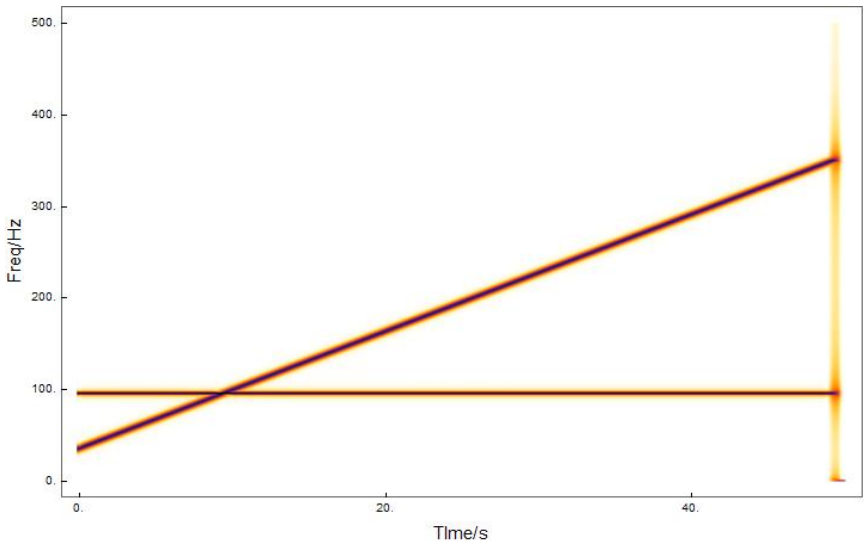

Figure A.1: A example of spectrogram

In this spectrogram, within a time range of $10s$ there are two lines, one horizontal line at around $100Hz$ and one ramp line starting at around $30hz$ and ending at around $370Hz$, which represent the $Sin(600t)$ and $Sin((200 + 20t)t)$ components respectively .

B

Equipments specs

Mechanical and electric property of these two piezo bender

B.1. Piezo bender

Technical Data

Model	P-876.A12	P-876.A15	Tolerances
Operating voltage	-100 to +400 V	-250 to +1000 V	
Motion and positioning			
Lateral contraction, open-loop	650 µm/m 1.3 µm/m/V	800 µm/m 0.64 µm/m/V	min. (+20 %/-0) min. (+20 %/-0)
Mechanical properties			
Blocking force	265 N	775 N	
Length	61 mm	61 mm	±0.5 mm
Width	35 mm	35 mm	±0.5 mm
Thickness	0.5 mm	0.8 mm	±0.5 mm
Bending radius	20 mm	70 mm	max.
Drive properties			
Ceramic type	PIC 255 Layer thickness: 200 µm	PIC 255 Layer thickness: 500 µm	
Electrical Capacitance	90 nF	45 nF	±20 %
Miscellaneous			
Operating temperature range*	-20 to +150 °C	-20 to +150 °C	
Mass	3.5 g	7.2 g	±10 %
Voltage connection	Soldering pads	Soldering pads	
Recommended controller / amplifier (actuator mode)	E-413.D2 (s. p. 2-120) E-835 (s. p. 2-166)	E-508 (s. p. 2-150) E-835 (s. p. 2-166)	

* Short-term operation up to 180 °C

Figure B.1: Piezo bender specification

Dimension of these two piezo bender is shown in figure below, geometric datas are the same expect for thickness which is already list above.

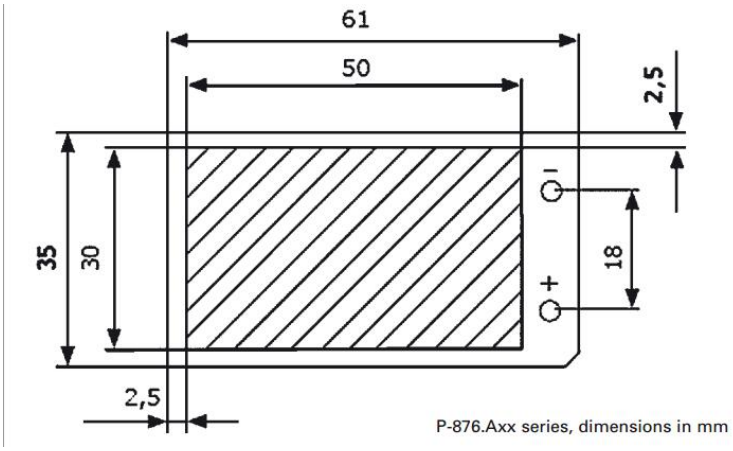

Figure B.2: Piezo bender size

Property of piezo ceramic PIC255 used in these piezo bender

Material type			PIC 255
Parameter			
Physical and dielectric properties			
Density	ρ	(g/cm³)	7.80
Curie temperature	Tc	(°C)	350
Permittivity in the polarization direction	$\varepsilon_{33}^T/\varepsilon_0$		1750
Permittivity perpendicular to the polarity	ε	ε	1650
Dielectric loss factor	tanδ		20
Electromechanical properties			
Coupling factors	k_p		0.62
	k_t		0.47
	k_{31}		0.35
	k_{33}		0.69
	k_{15}		0.66
Piezoelectric charge constants	d_{31}	(10^{-12} C/N)	-180
	d_{33}		400
	d_{15}		550
Piezoelectric voltage constants	g_{31}	(10^{-3} Vm/N)	-11.3
	g_{33}		25
Acousto-mechanical properties			
Frequency constants	N_p	(Hzm)	2000
	N_1		1420
	N_3		
	N_t		2000
Elastic constants (compliance)	S_{11}^E	(10^{-12} m²/N)	16.1
	S_{33}^E		20.7
Elastic constants (stiffness)	C_{33}^D	(10^{10} N/m²)	
Mechanical quality factor	Qm		80
Temperature stability			
Temperature coefficient of ε_{33} (in the range -20°C up to +125°C)	TK ε_{33}	(x10^{-3}/K)	4
Aging stability (relative change of the parameter per decade in %)			
Relative dielectric constant	C	(%)	-1.0
Coupling factor	C_K		-1.0

Figure B.3: Property of PIC255 material

B.2. Amplifier

Voltage Output Range	-500 V to +1500 V, SHV connector, 200 V/V for wave generator input, noninverting,
Current Output Range	0 to +/- 50 mA DC, 0 to 60mA peak AC
Bandwidth	large signal bandwidth (-3dB) DC to 10kHz
Slew Rate	greater than 50 V/µs
External Voltage Control Input	-2.5 V to +7.5 V corresponds to -500 V to +1500 V output, input impedance 100 kΩ, BNC coaxial connector
External Voltage Audio Control Input	0.2 V to 3 V AC, Input Resistance 100 kΩ Gain Control Range -12 db to +12db, by using a 10-turn potentiometer, Offset Control Range -500 V to +1500 V, by using a 10-turn potentiometer, Signal Frequency Range 10 Hz to 10 kHz Connector BNC coaxial connector
High Voltage Monitor Output	BNC, 1/200 of the High Voltage Output, output impedance 1kOhm
Current Monitor Output	BNC, 0.2V/mA, output impedance 1kOhm
Main Input	115/230VAC, 50/60 Hz, 150VA
Compliance	Œ, EN 50081-1; EN 50082 or EN50081-2; EN 50082-2

Figure B.4: Amplifier specification

B.3. Laser Sensor

Type ILD1402-5 and ILD 1402-20 LDS are used in this project.

Model		ILD 1402-5(025)	ILD 1402-10(025)	ILD 1402-20(025)	ILD 1402-50(025)	ILD 1402-100(025)	ILD 1402-200(025)	ILD 1402-400(025)	ILD 1402-600(025)
Measuring range		5mm	10mm	20mm	50mm	100mm	200mm	400mm	600mm
Start of measuring range		20mm	20mm	30mm	45mm	50mm	60mm	200mm	200mm
Midrange		22.5mm	25mm	40mm	70mm	100mm	160mm	400mm	500mm
End of measuring range		25mm	30mm	50mm	95mm	150mm	260mm	600mm	800mm
Linearity [1]		5...9µm	5...18µm	7...36µm	12...90µm	20...180µm	40...360µm	120...1200µm	120...3000µm
		≤0.18% FSO						≤0.5% FSO	
Resolution [2]	averaged with averaging factor 64	0.6µm	1µm	2µm	5µm	10µm	13µm	80µm	80µm
		0,01% FSO.							
	dynamic 1.5 kHz	1...3µm	2...5µm	5...10µm	6...25µm	12...50µm	13...100µm	80...480µm	80...600µm
		0.02...0.05% FSO						0.02...0.12% FSO	
Measuring rate, programmable		1.5kHz; 1kHz; 750Hz; 375Hz; 50Hz							
Light source		semiconductor laser <1mW, 670nm (red)							
Laser safety class		class 2 IEC 60825-1 : 2008-05							
Spot diameter	SMR	110µm	110µm	210µm	1100µm	1400µm	2300µm	2.6 x 5mm	2.6 x 5mm
	MMR	380µm	650µm	530µm	110µm	130µm	2200µm	2.6 x 5mm	2.6 x 5mm
	EMR	650µm	1200µm	830µm	1100µm	1400µm	2100µm	2.6 x 5mm	2.6 x 5mm
Protection class		IP 67							
Vibration		15g / 10Hz ... 1kHz							
Shock		15g / 6ms (IEC 68-2-29)							
Weight (without cable)		appr. 83g						appr. 130g	
Operation temperature		0 ... +50°C							
Storage temperature		-20 ... +70°C							
Measurement output	analogue	4 ... 20mA (1 ... 5V with cable PC 1401-3/U); free scalable within the nominal range							
	digital	RS232 / 14bit							
Control I/O		1x open collector output (switching output, switch, error); 1x input (teach in, trigger); 1x laser on/off							
Supply		11 ... 30VDC, 24VDC / 50mA							
Controller		integrated signal processor							
Software		free setup and aquisition tool + SDK (software development kit)							
Electromagnetic compatibility (EMC)		EN 61326-1:2006 / EN 55011 Class B (Interface emission) EN 61326-1:2006 / EN 61000-4-2:1995 + A1:1998 + A2:2001 (Interference resistance)							

Figure B.5: Sensor specifications

B.4. Piezo bender identification setup dimensions

Clamping detail and sensor measuring point are shown in figure below, distance between two areas following dimension detail shown in figure B.2

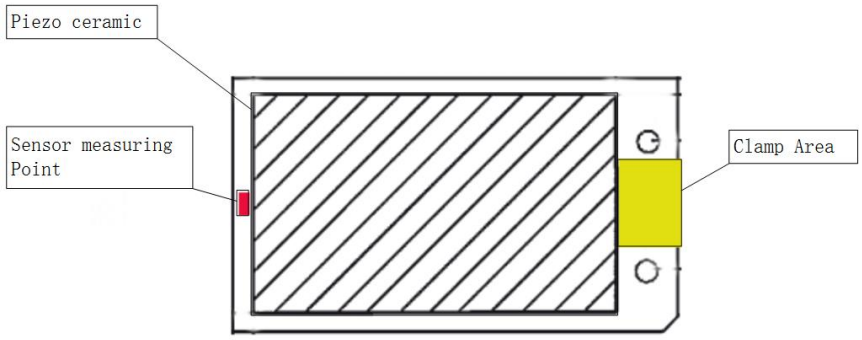

Figure B.6: Pizeo bender identification setup configuration

B.5. Complete prototype identification setup dimensions

Key size of prototype identification setup

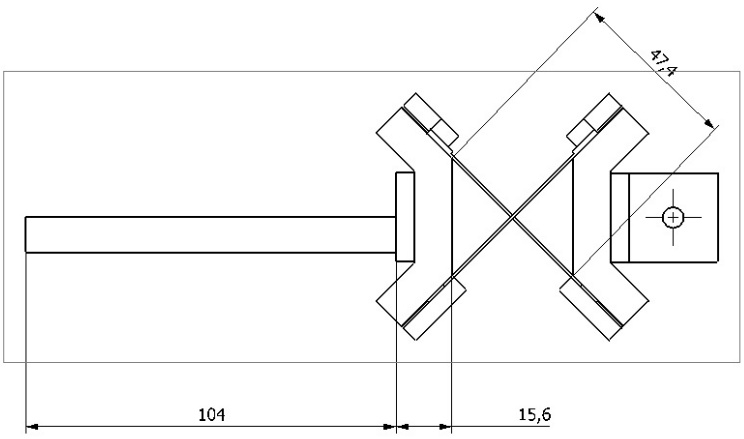

Figure B.7: Pizeo bender identification setup configuration

C

Mathematica code used for identification

```
GetBodePlot[input_, output_, Samplerate_, option_] :=
 Module[{in = input, out = output, samplerate = Samplerate, opt = option,
   n, sain, saout, absain, absaout, windown, window, scal, inpeaks, peakpos1,
   rawgain, rawphase, gain, rawphase2, phase, r1, rawphase3, , rawphase4,
   plength, pgain, pphase, outpeaks, peakpos2, zeros, coherence},
  n = Length[in];
  sain = SpectrogramArray[in - Mean[in]];
  saout = SpectrogramArray[out - Mean[out]];
  absain = Abs[sain];
  absaout = Abs[saout];
  windown = Length[sain];
  window = Length[sain[[1]]];
  scal = samplerate / window;
  Parallelize[
   inpeaks = Table[FindPeaks[absain[[n, 1 ;; window - 3]], 10], {n, 1, windown, 1}];
  ];
  (*Parallelize[
    outpeaks=Table[FindPeaks[absaout[[n,1;;window-3]],10],{n,1,windown,1}];
   ];*)
  Parallelize[peakpos1 =
     Table[inpeaks[[n, Round[FindPeaks[Transpose[inpeaks[[n]]][[2]]][[1, 1]] - 0.1],
       1]], {n, 1, Length[sain], 1}];];
  (*Parallelize[peakpos2=Table[outpeaks[[n,
        Round[FindPeaks[Transpose[outpeaks[[n]]][[2]]][[1,1]]-0.1],
        1]],{n,1,Length[sain],1}];];*)
  rawgain = Table[absaout[[n, peakpos1[[n]]]] / absain[[n, peakpos1[[n]]]],
    {n, 1, windown, 1}];
  rawphase = Table[-Arg@sain[[n, peakpos1[[n]]]] + Arg@saout[[n, peakpos1[[n]]]],
    {n, 1, windown, 1}];
  gain = Sort[Partition[Riffle[peakpos1 * scal, rawgain], 2]];
  (*rawphase2=Mod[rawphase+20*Pi,2Pi];*)
  rawphase2 = Sort[Partition[Riffle[peakpos1 * scal, Mod[rawphase + 20 * Pi, 2 Pi]], 2]];
  r1 = Split[Transpose[rawphase2][[2]], Abs[#1 - #2] < 5 &];
  rawphase3 = r1[[-1]];
  plength = 2^(Round[Log[2, Length[gain]]] + 1);
  (*For[nn=Length[r1],nn>1,nn--,
    If[
     rawphase3[[1]]>3.5,
     rawphase3=Join[r1[[nn-1]],rawphase3-2*Pi],
     rawphase3=Join[r1[[nn-1]]],rawphase3+2*Pi
    ]];*)
  For[nn = Length[r1], nn > 1, nn--,
   If[
    rawphase3[[1]] > 3.5,
    {rawphase3 = Join[r1[[nn - 1]], rawphase3 - 2 * Pi]},
    {rawphase3 = Join[r1[[nn - 1]], rawphase3 + 2 * Pi]}
   ]];
  rawphase4 = rawphase3 + (Mod[rawphase3[[50]] + 20 Pi, 2 Pi] - rawphase3[[50]]);
  phase = Sort[Partition[Riffle[Sort[peakpos1 * scal], rawphase4], 2]];
  plength = 2^(Round[Log[2, Length[gain]]] + 1);
  pgain = ListLogLinearPlot[gain, opt, AxesLabel → {"f/Hz", "dB"},
    Joined -> True, PlotLabel → "Gain" , PlotRange → {{1, plength}, All}];
  pphase = ListLogLinearPlot[phase, opt, AxesLabel → {"f/Hz", ""},
    Joined → True, PlotLabel → "Phase" , PlotRange → {{1, plength}, All}];
```

```
 (*Grid[{{pgain},{pphase}}]*)
 zeros = Table[0, {n, 1, 25, 1}];
 coherence = Table[(Join[zeros, absain[[n]]][[peakpos1[[n]] ;; peakpos1[[n]] + 50]].
       Join[zeros, absaout[[n]]][[peakpos1[[n]] ;; peakpos1[[n]] + 50]])^2 /
    (Join[zeros, absain[[n]]][[peakpos1[[n]] ;; peakpos1[[n]] + 50]].
       Join[zeros, absain[[n]]][[peakpos1[[n]] ;; peakpos1[[n]] + 50]] *
      Join[zeros, absaout[[n]]][[peakpos1[[n]] ;; peakpos1[[n]] + 50]].
       Join[zeros, absaout[[n]]][[peakpos1[[n]] ;; peakpos1[[n]] + 50]]),
   {n, 1, Length[absain], 1}];
 coherence = Sort[Partition[Riffle[peakpos1 * scal, coherence], 2]];
 {gain, phase, coherence}
]
```

```
model = n / ((s^2 + a * s + b) * (s^2 + c * s + d)) / (s + e);
par = {n, a, b, c, d, e};

initial = Partition[Riffle[par, {250 000 000, 5, 10 000, 5, 250 000, 100}], 2];
fitdataA1 = sAB[[1]].{{2 Pi, 0}, {0, 1}};
fitdataA2 = Split[fitdataA1, #1[[1]] > 10 &];
fitresA = NonlinearModelFit[
   fitdataA2[[-1]][[1 ;; 600]], Norm[model /. s → (w * I)], initial, w];
fitresA["ParameterTable"]
ListLogLinearPlot[fitresA[{"Response", "PredictedResponse"}], PlotRange → All]

res = Transpose[fitresA["ParameterTable"][[1, 1]]][[2, 2 ;;]]

fmodel = model /. Thread[par → res];
model2 = n / ((s^2 + a * s + b) * (s^2 + c * s + d));
fgain = Table[{w / 2 / Pi, Norm[fmodel /. s → (w * I)]}, {w, 0, 830, 1}];
fphase = Table[{w / 2 / Pi, Mod[Arg[fmodel /. s → (w * I)] + 6 Pi, 2 Pi]}, {w, 0, 800, 1}];

f1 = ListLogLogPlot[{fgain, sAB[[1]]}, PlotRange → {{1, 150}, {0.001, 10}},
  ImageSize → 720, AxesLabel → {"Freq/Hz", "Magnitude/dB"}, Joined → True,
  Background → Lighter[Gray, 0.9], GridLines → {All, Automatic},
  PlotLegends → Placed[{"Fit result", "Original data"}, {Bottom, Right}]]
f2 = ListLogLinearPlot[{fphase, sAB[[2]]}, PlotRange → {{1, 150}, All},
  ImageSize → 720, AxesLabel → {"Freq/Hz", "Phase/rad"}, Joined → True,
  Background → Lighter[Gray, 0.9], GridLines → {All, Automatic},
  PlotLegends → Placed[{"Fit result", "Original data"}, {Bottom, Right}]]
```

D

Experiments result

D.1. Nonlinearity classification

Piezo bender identification process indicates that these piezo bender meet serious nonlinearity. Features of nonlinearity of the two piezo bender are similar and can be classified into thre category. In order to have a clear view of these nonlinearity, spectrograms have been post-processed to have acheive a higher contrast.

D.1.1. Harmony effect

For both types of piezo bender harmony effect is the strongest nonlinear source because it affects not only the input signal but also other disturbance source. As marked as red in figures, there are much more ramp line in the output spectrogram, and lopes of these extra lines are exactly twice, three times, etc higher than that of input line.

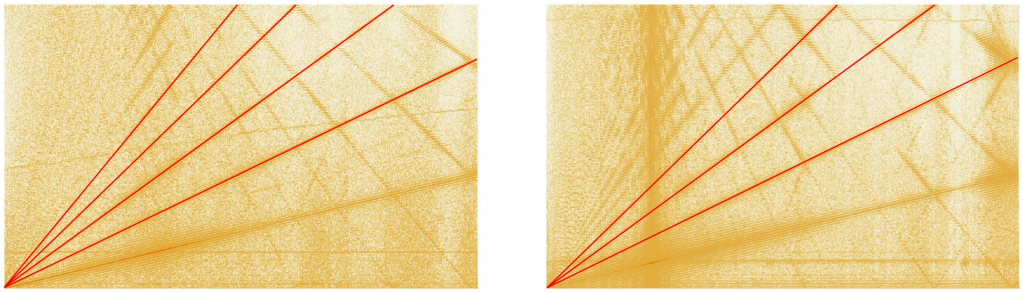

(a) A15 piezo (b) A12 piezo

Figure D.1: Harmony affect on input signal

D.1.2. Constant disturbance

As marked as blue in figures below, these horizontal lines represent constant frequency components. Considering that frequency and amplitude of this disturbance do not change with time,power grid disturbance source such as a unfiltered wall outlet could one reason. Besides, white noise of the input signal also excite the eigen mode, so there is one horizontal line around the eigen frequency. As mention in previous section, this disturbance is also affected by harmony effect.

(a) A15 piezo (b) A12 piezo

Figure D.2: Grid type disturbance

D.1.3. Coupling effect

As marked as Green in figures, these curves appear no matter if load presents or not and its shape laso changed with different load condition. Such kind of disturbance should be the result of amplifier itself.

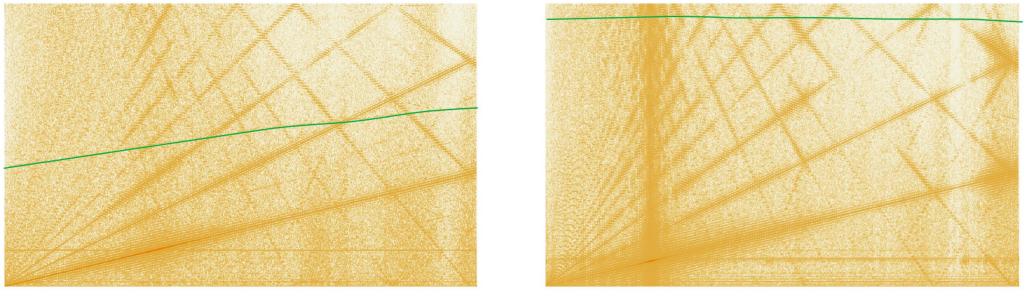

(a) A15 piezo (b) A12 piezo

Figure D.3: Coupling effect

Bibliography

[1] Jung W S, Kang M G, Moon H G, et al. *High output piezo/triboelectric hybrid generator*. Scientific reports, 2015, 5: 9309.

[2] Spadoni A, Ruzzene M, Cunefare K. *Vibration and wave propagation control of plates with periodic arrays of shunted piezoelectric patches*. Journal of Intelligent Material Systems and Structures, 2009, 20(8): 979-990.

[3] Tzou H S, Tseng C I. *Distributed vibration control and identification of coupled elastic/piezoelectric systems: finite element formulation and applications*. Mechanical Systems and Signal Processing, 1991, 5(3): 215-231.

[4] Mottard P, St-Amant Y. *Analysis of flexural hinge orientation for amplified piezo-driven actuators*. Smart Materials and Structures, 2009, 18(3): 035005.

[5] Xu S X, Koko T S. *Finite element analysis and design of actively controlled piezoelectric smart structures*. Finite elements in analysis and design, 2004, 40(3): 241-262.

[6] Kay S M, Marple S L. *Spectrum analysis—a modern perspective*. Proceedings of the IEEE, 1981, 69(11): 1380-1419.

[7] Kwon H S, Kim Y H. *Minimization of bias error due to windows in planar acoustic holography using a minimum error window*. The Journal of the Acoustical Society of America, 1995, 98(4): 2104-2111.

[8] Ha Y H, Pearce J A. *A new window and comparison to standard windows*. IEEE Transactions on Acoustics, Speech, and Signal Processing, 1989, 37(2): 298-301.

[9] XU Q, TAN K.K *Advanced control of piezoelectric micro-/nano positioning system* ,Springre, ISSN 1430-9491

[10] Kerschen G, Worden K, Vakakis A F, et al. *Past, present and future of nonlinear system identification in structural dynamics*. Mechanical systems and signal processing, 2006, 20(3): 505-592.

[11] Gaudenzi P, Carbonaro R, Benzi E. *Control of beam vibrations by means of piezoelectric devices: theory and experiments*. Composite structures, 2000, 50(4): 373-379.

[12] Alam M S, Tokhi M O. *Designing feedforward command shapers with multi-objective genetic optimisation for vibration control of a single-link flexible manipulator*. Engineering Applications of Artificial Intelligence, 2008, 21(2): 229-246.

[13] Schmidt P, Rehm T. *Notch filter tuning for resonant frequency reduction in dual inertia systems* Industry Applications Conference, 1999. Thirty-Fourth IAS Annual Meeting. Conference Record of the 1999 IEEE. IEEE, 1999, 3: 1730-1734.

[14] Beker, Orhan and Hollot, CV and Chait, Yossi and Han, Huaizhong, *Fundamental properties of reset control systems*, IEEE Transactions on Automatic Control, 2001, 46(11): 1797-1799.

[15] Wu D, Guo G, Wang Y. *Reset integral-derivative control for HDD servo systems*, IEEE Transactions on Control Systems Technology, 2007, 15(1): 161-167.

[16] Tesfaye, Addisu and Lee, Ho Seong and Tomizuka, Masayoshi, *A sensitivity optimization approach to design of a disturbance observer in digital motion control systems*, IEEE/ASME Transactions on mechatronics, 2000, 5(1): 32-38.

[17] Kempf C J, Kobayashi S. *Disturbance observer and feedforward design for a high-speed direct-drive positioning table*. IEEE Transactions on control systems Technology, 1999, 7(5): 513-526.